HHS Public Access

Author manuscript

J Comp Neurol. Author manuscript; available in PMC 2021 April 01.

Published in final edited form as:

J Comp Neurol. 2020 April 01; 528(5): 840–864. doi:10.1002/cne.24783.

Expression of Protocadherin-γC4 protein in the rat brain

Celia P. Miralles, **Michael J. Taylor**, **John Bear Jr.**[1], **Christopher D. Fekete**, **Shanu George**, **Yanfang Li**[2], **Bevan Bonhomme**[3], **Tzu-Ting Chiou**[4], **Angel L. De Blas**[*]

Department of Physiology and Neurobiology, University of Connecticut, Storrs, Connecticut, 06269, USA.

Abstract

It has been proposed that the combinatorial expression of γ-protocadherins (Pcdh-γs) and other clustered protocadherins (Pcdhs) provides a code of molecular identity and individuality to neurons, which plays a major role in the establishment of specific synaptic connectivity and formation of neuronal circuits. Particular attention has been directed to the Pcdh-γ family, for which experimental evidence derived from Pcdh-γ-deficient mice shows that they are involved in dendrite self-avoidance, synapse development, dendritic arborization, spine maturation and prevention of apoptosis of some neurons. Moreover, a triple-mutant mouse deficient in the three C-type members of the Pcdh-γ family (Pcdh-γC3, Pcdh-γC4 and Pcdh-γC5) shows a phenotype similar to the mouse deficient in whole Pcdh-γ family, indicating that the latter is largely due to the absence of C-type Pcdh-γs. The role of each individual C-type Pcdh-γ is not known. We have developed a specific antibody to Pcdh-γC4 to reveal the expression of this protein in the rat brain. The results show that although Pcdh-γC4 is expressed at higher levels in the embryo and earlier postnatal weeks, it is also expressed in the adult rat brain. Pcdh-γC4 is expressed in both neurons and astrocytes. In the adult brain, the regional distribution of Pcdh-γC4 immunoreactivity is similar to that of Pcdh-γC4 mRNA, being highest in the olfactory bulb, dentate gyrus and cerebellum. Pcdh-γC4 forms puncta that are frequently apposed to glutamatergic and GABAergic synapses. They are also frequently associated with neuron-astrocyte contacts. The results provide new insights into the cell recognition function of Pcdh-γC4 in neurons and astrocytes.

[*]**Corresponding author:** Dr. Angel L. De Blas, Department of Physiology and Neurobiology, University of Connecticut, 75 North Eagleville Road, U-3156, Storrs, Connecticut, 06269-3156, USA, angel.deblas@uconn.edu, Tel. 1-860-486-5440, Fax. 1-860-486-5439.

[1]Present address: John Bear Jr., School of Life Sciences, University of Sussex, Brighton BN1 9QG, UK.

[2]Present address: Fujian Provincial Key Laboratory of Neurodegenerative Disease and Aging Research, Institute of Neuroscience, School of Medicine, Xiamen University, Xiamen 361005 Fujian, China

[3]Present address: New York Medical College, 40 Sunshine Cottage Road, Valhalla, NY 10595, USA

[4]Present address: University of California, Los Angeles, 650 Charles E Young Drive South, Room A2-422 MDCC, Los Angeles, California, 90095-8347, USA

ROLE OF AUTHORS

Study concept and design: A.L.D. Study supervision: C.P.M., C.F. and A.L.D. Acquisition of data: C.P.M., Y.L., J.B.J., M.J.T., C.F., S.G., T-T.C., B.B. Analysis and interpretation of data: C.P.M., Y.L., J.B.J., M.J.T., C.F., S.G., T-T.C, B.B. and A.L.D. Drafting of the manuscript: A.L.D. Critical revision of the manuscript for important intellectual content: C.P.M., S.G. and A.L.D. Obtained funding: A.L.D.

CONFLICT OF INTEREST

The authors declare no financial conflict of interest.

DATA AVAILABILITY STATEMENT

The data that support the findings of this study are available from the corresponding author upon reasonable request

Keywords

astrocytes; synapse formation; GABAergic synapse; glutamatergic synapse; protocadherins; neuron-astrocyte interaction; cell-cell recognition; RRID:AB_10676098; RRID:AB_10672982; RRID:AB_2259153; RRID:AB_1279448; RRID:AB_2314493; RRID:AB_2313650; RRID:AB_2092365; RRID:AB_887873; RRID:AB_2301751; RRID:AB_477499; RRID:AB_2223041

INTRODUCTION

Clustered protocadherins (Pcdhs) are transmembrane cell-adhesion proteins of the cadherin superfamily that are predominantly expressed in the CNS. They are involved in neuron-neuron and neuron-glia recognition events which includes dendrite arborization, spine maturation, axon tiling, dendrite self-avoidance, formation and function of neural circuits, synaptic development and prevention of apoptosis of some interneurons (W. V. Chen & Maniatis, 2013; Hasegawa et al., 2017; Hayashi & Takeichi, 2015; Hirayama & Yagi, 2013, 2017; Keeler, Molumby, & Weiner, 2015; Molumby et al., 2017; Molumby, Keeler, & Weiner, 2016; Mountoufaris, Canzio, Nwakeze, Chen, & Maniatis, 2018; Peek, Mah, & Weiner, 2017; Weiner & Jontes, 2013). In mice there are 58-clustered Pcdhs distributed in three families: alpha (Pcdh-α), beta (Pcdh-β) and gamma (Pcdh-γ), having 14, 22 and 22 members respectively. They are called clustered Pcdhs because the genes of the three families are arranged in tandem, in a small locus of a single chromosome (Wu, 2005; Wu & Maniatis, 1999; Wu et al., 2001).

Different neurons express unique combinations of Pcdh-αs, Pcdh-βs and Pcdh-γs, by a mechanism of random and combinatorial transcription (W. V. Chen & Maniatis, 2013; Esumi et al., 2005; Kaneko et al., 2006; Tasic et al., 2002; Wang et al., 2002; Wu & Maniatis, 1999). The stochastic expression of Pcdhs may provide molecular identity and individuality to neurons. Although the large majority of clustered Pcdhs are stochastically expressed, the five C-type Pcdhs members, two of the Pcdh-α family (Pcdh-αC1 and Pcdh-αC2) and three of the Pcdh-γ family (Pcdh-γC3, Pcdh-γC4 and Pcdh-γC5) are constitutively expressed in many, but not all neurons (Esumi et al., 2005; Frank et al., 2005; Hirano et al., 2012; Hirayama & Yagi, 2017; Kaneko et al., 2006). It is worth noting olfactory sensory neurons (OSN) don’t express C-type Pcdhs (Mountoufaris et al., 2017).

The set of clustered Pcdhs expressed by a single cell, promiscuously interact in cis forming cis-heteromeric complexes (Biswas, Emond, & Jontes, 2012; Schreiner & Weiner, 2010; Thu et al., 2014). In contrast, trans-interactions require homophilic matching of the isoform complexes (Lefebvre, 2017; Schreiner & Weiner, 2010; Thu et al., 2014; Yagi, 2012; Zipursky & Sanes, 2010), which could lead to: i) selective recognition and increased adhesion between two matching cells that express identical Pcdh complexes regulating dendritic arborization; ii) decreased adhesion between matching dendrites from the same neuron (dendrite self-avoidance) and iii) axon repulsion from different neurons (axon tiling) (W. V. Chen et al., 2017; Mountoufaris et al., 2018; Mountoufaris et al., 2017).

The mouse KO that is deficient in all members of the Pcdh-γ family (GKO) dies at birth and shows a severe loss of interneurons in spinal cord and retina, suggesting that Pcdh-γs prevent neuronal apoptosis of some neurons (W. V. Chen et al., 2012; Lefebvre, Zhang, Meister, Wang, & Sanes, 2008; Prasad, Wang, Gray, & Weiner, 2008; Wang et al., 2002; Weiner, Wang, Tapia, & Sanes, 2005). A triple knockout (TCKO) mouse has been generated (W. V. Chen et al., 2012), in which the three C-type members of the C-type Pcdh-γ family (Pcdh-γC3, Pcdh-γC4 and Pcdh-γC5) have been deleted. The TCKO mouse is phenotypically similar to the GKO mouse that lacks the whole Pcdh-γ cluster, in that both show neuronal losses in spinal cord and retina and perinatal death of these mutants at P0 (W. V. Chen et al., 2012). To the best of our knowledge, no individual Pcdh-γC type KO mice have been produced or characterized and therefore, the functional role of each individual Pcdh-γCs is not well understood. In an effort to understand the role of individual Pcdh-γCs, we have previously studied the expression of Pcdh-γC5 protein in brain (Y. Li et al., 2010; Y. Li et al., 2012). In the present communication, we have made a novel anti-Pcdh-γC4 antibody to characterize the patterns of expression and localization of Pcdh-γC4 protein in the brain, neurons and astrocytes.

MATERIALS AND METHODS

Animals

All the animal protocols have been approved by the Institutional Animal Care and Use Committee of the University of Connecticut and have followed the National Institutes of Health guidelines. Both male and female rat and mice were used in the experiments. Most experiments were done with Sprague-Dawley rat brain tissue, but when indicated, we used the triple C-type Pcdh-γ knockout (TCKO) mouse brain for immunoblots (Fig. 4) and neuronal cultures (Fig. 6). The TCKO mouse is deficient in the three C-type Pcdh-γs (Pcdh-γC3, Pcdh-γC4, and Pcdh-γC5), but expresses the other types of Pcdh-γs. The generation and characterization of this mouse has been previously described (W. V. Chen et al., 2012). The TCKO dies soon after birth but for some experiments we have prepared neuronal cultures from TCKO mouse embryos. Rat and mouse embryos of either sex were used for hippocampal neuronal cultures. Female rats were used for preparing rat brain homogenates and membranes.

Antibodies and plasmids.

Table I summarizes the primary antibodies used in this communication.

A novel rabbit (Rb) antibody was raised to a synthetic peptide corresponding to an amino acid (AA) sequence unique to Pcdh-γC4 (DHAPRFPRQQLDLE), as determined from Entrez protein database. This peptide AA sequence is localized at the variable extracellular domain and is identical in rat, human and mouse Pcdh-γC4. The peptide sequence is localized in AA residues 128–141 in the rat, 131–144 in the mouse, and 128–141 in human Pcdh-γC4 deduced protein sequences. The GenBank accession numbers are NM_033582.2 for mouse and NM_018928.2 for human. The rat Pcdh-γC4 sequence was derived from the rat genomic sequence (AC113777.5 HTGS High-Throughput Genome Sequencing, AC_000086 and NW_001084735.1). The Pcdh-γC4 protein, including the signal peptide,

has 938 AA in rat, 941 AA in mouse and 938 AA in human. Signal peptides are AA 1–29 in rat and human and AA 1–32 in mouse. The mature protein has 909 AA in the three species.

The aforementioned synthetic peptide was covalently coupled, via an added C-terminal cysteine, to keyhole limpet hemocyanin and antisera were collected from a New Zealand rabbit (Rb) four months after repeated immunizations. The antibody from the serum was affinity-purified on immobilized antigen peptide for all immunoblot, immunocytochemistry and immunofluorescence experiments.

The mouse (Ms) monoclonal antibody (mAb) to pan-Pcdh-γ to AA 808–931 of the constant cytoplasmic domain of mouse Pcdh-γA1 that is shared by all 22 Pcdh-γs (clone N159/5; catalog# 73–185; lot# 437–3VA-24; RRID: AB_10676098) and the Ms mAb to pan-Pcdh-γA to AAs 720–804 of the cytoplasmic domain of mouse Pcdh-γA3 that is similar in all Pcdh-γAs (clone N144/32; catalog # 73–178; Lot # 437–3VA-12: RRID: AB_10672982) were from NeuroMab (Davis, CA).

The Ms mAb to Pcdh8 to AA 1–149 of human Pcdh8 (clone 7, catalog# SC-377348, lot# 3E1817; RRID: AB_2299153) was from Santa Cruz Biotechnology (Dallas, TX).

The Ms anti-gephyrin mAb (clone mAb7a; catalog #147021; lot#147021/9; RRID: AB_1279448) and the guinea pig (GP) anti-VGAT (cat. no. 131004; lot no. 131004/13; RRID: AB_887873) were from Synaptic Systems (Gottingen, Germany). This antibody is in the JCN database.

The GP anti-rat vesicular glutamate transporter 1 (VGLUT1) (catalog #AB5905; lot# 24080852; RRID: AB_2301751), the Ms mAb to rat PSD-95 (clone 6G6–1C9; catalog #MAB1596, Lot# LV1453199; RRID: AB_2092365) and the Ms mAb to actin (clone C4; catalog # MAB1501; lot# LV1547855; RRID: AB_2223041) were from EMD Millipore (Billerica, MA). These antibodies are in the JCN antibody database.

The sheep (Sh) anti-GAD (lot #1440–4, RRID: AB_2314493) was a gift from Dr. Irwin J. Kopin (NINDS, National Institutes of Health, Bethesda, MD). This antibody recognizes a 65-kDa protein band in rat brain immunoblots. The antibody precipitated GAD from rat brain and detected purified GAD in crossed immunoelectrophoresis (Oertel, Schmechel, Mugnaini, Tappaz, & Kopin, 1981; Oertel, Schmechel, Tappaz, & Kopin, 1981). This antibody is in the JCN antibody database.

The Ms mAb anti-glial fibrillary acidic protein, GFAP (clone 4A11; catalog# 60311D, lot number MO50728; RRID: AB_2313650) was from Pharmingen (San Diego, CA). The Ms mAb anti-S-100 (β-subunit) to bovine S-100β (clone SH-B1; catalog # S2532; lot#85K4880 and catalog # AB4200671; RRID: AB_477499) was from Sigma (St. Louis, MO). Chicken polyclonal anti PSD-95 (to a GST fusion protein encoding the full-length rat PSD-95, RRID: AB_2315222), was a gift from Dr. Randall S. Walikonis (University of Connecticut, Storrs, CT). These antibodies are is in the JCN antibody database.

For immunofluorescence in cell cultures, fluorophore-labeled fluorescein isothiocyanate (FITC), DyLight 594 or Alexa Fluor 594, or aminomethylcoumarin (AMCA) species-

specific anti-IgG antibodies were made in donkey (Jackson Immunoresearch Laboratories, West Grove, PA). For confocal microscopy the species-specific anti-IgG secondary antibodies were raised in goat and labeled with Alexa Fluor 488, 568 or 647 (Invitrogen, Eugene, OR).

For Pcdh expression in HEK293 cells, the following plasmids were used: i) pEGFP-N1 for Pcdh-γC3-EGFP (Frank et al., 2005) and Pcdh-γC5-EGFP (Y. Li et al., 2012); ii) pMaxcherry for Pcdh-γC4-mCherry expression (Thu et al., 2014); iii) pcDNA3.1(+) for ^{cmyc}Pcdh-γC5 (Y. Li et al., 2012) and Pcdh8. The Pcdh8 (GenBank accession number BC053008) plasmid was subcloned from pYX-Ascp-Pcdh8 (from PlasmID repository, ID MmCD00319448, Harvard Medical School, Boston, MA) in the EcoRI and NotI sites of pcDNA3.1(+) and iv) the pEF6-mCherry vector was a gift from Dr. David Knecht, University of Connecticut (Storrs, CT).

Brain fractionation and Immunoblots.—All steps were performed at 4°C. Homogenates were prepared from pooled forebrains (telencephalon) of male and female rats of the same age, by homogenization with a glass/Teflon homogenizer (1g of tissue) in10ml of 10% sucrose, 50mM Tris-HCl pH 7.4, containing 1mM phenylmethylsulfonyl fluoride and a cocktail of protease inhibitors (Roche, Indianapolis, IN). The homogenate was centrifuged at 1,000×g for 10 min (to pellet nuclei and cell debris) and the supernatant (cleared homogenate) was used for immunoblots. Additionally, brain membranes were prepared from cleared homogenates from adult rats by centrifugation at 100,000×g for 1hr, followed by pellet suspension in 5mM Tris-HCl pH 7.4, homogenization in a glass Dounce homogenizer, centrifugation at 12,000×g for 30 min and suspension of the pellet in 50mM Tris-HCl pH 7.4. Cleared homogenates from mouse brain were prepared as for rat brain except that the whole brain was used. The protein concentrations of different brain fractions were measured by using Micro BCA Protein Assay Reagent Kit (Pierce, Rockford, IL).

Immunoblots were a modification of the procedure previously described (De Blas & Cherwinski, 1983), using IRDye 800CW- or 680LT-conjugated goat anti-rabbit or anti-mouse IgG secondary antibodies from Li-Cor Biosciences (Lincoln, NE). Immunoblot images were collected with a LI-COR Odyssey Infrared Imaging System (Li-Cor Biosciences).

Cell culture immunofluorescence.—Rat hippocampal (HP) neuronal cultures were prepared according to Higgins and Banker (1998) as described elsewhere (Chiou et al., 2011; Christie & de Blas, 2002, 2003; Christie, Li, et al., 2002; Christie, Li, Miralles, Yang, & De Blas, 2006; Jin et al., 2014). Briefly, dissociated neurons from embryonic day 18 (E18) rat hippocampi (from Sprague Dawley embryos of either sex) were plated (at a density of 3000–8000 cells per 18 mm diameter poly-L-lysine coated glass coverslip) and maintained in rat glial cell conditioned medium for 21 days. Mouse HP cultures were prepared from E18 embryos of either sex as described above for rat, and maintained in rat glial cell conditioned medium. Astrocyte cultures were prepared from the cerebral cortex of postnatal day 0 (P0) Sprague Dawley (SD) rats according to Higgins and Banker (1998) as described elsewhere (Y. Li et al., 2010) and plated on 18 mm diameter poly-L-lysine coated glass coverslips. Cultured human embryonic kidney cell line 293 (HEK293) were

transfected with 2 μg of plasmid using the CalPhos Mammalian Transfection Kit according to the instructions provided by the manufacturer (BD Bioscience, San Jose, CA). Immunofluorescence of HEK293 cells was performed 3 days after transfection.

Immunofluorescence of HP, glial or HEK293 cultures was performed as described elsewhere (Christie, Li, et al., 2002; Christie et al., 2006; Christie, Miralles, & De Blas, 2002; Y. Li et al., 2010). HEK293 cells were from ATCC (ATTC Cat# CRL-1573, RRID: CVCL_0045). Briefly, cells on glass coverslips were fixed with 4% paraformaldehyde, 4% sucrose in 0.1 M phosphate buffered saline (PBS) for 15 minutes. The free aldehyde groups were quenched with 50mM NH_4Cl in PBS for 10min. Permeabilization was done with 0.25% Triton X-100 in PBS (T-PBS) for 5 minutes, followed by incubation with 5% normal donkey serum (NDS) in T-PBS for 30 min. Incubations with primary and secondary antibodies were done in T-PBS containing 2% NDS. For surface labeling, live cells were incubated with the primary antibody at 37°for 30 min followed by washes, fixation and permeabilization. The coverslips were mounted on glass slides with Prolong Gold anti-fade mounting solution (Invitrogen, Eugene, OR).

Immunocytochemistry of rat brain sections.—This procedure has been described elsewhere (Charych, Yu, Li, et al., 2004; Charych, Yu, Miralles, et al., 2004; de Blas, 1984). Briefly, 35-day old SD rats from either sex were deeply anesthetized with a mixture of ketamine-HCl/xylazine (100/10 mg/kg) and perfused through the ascending aorta with 0.12M phosphate buffer (PB, 27mM NaH_2PO_4, 92mM Na_2HPO_4, pH 7.4) followed by 4% PLP fixative (4% paraformaldehyde, 1.37% lysine, 0.21% sodium periodate in 0.12M phosphate buffer, pH 7.4). Brains were cryoprotected, frozen and sectioned (25μm thick) with a freezing microtome.

Free-floating parasagittal sections were incubated with the anti-Pcdh-γC4 antibody in 0.3% Triton X-100 in PB at 4°C overnight followed by incubation with biotinylated anti-rabbit IgG and avidin-biotin-horseradish peroxidase complex (ABC procedure, Vectastain Elite ABC Kit, Vector Laboratories, Burlingame, CA) in 1% normal goat serum. Sections were then incubated with 3–3’ diaminobenzidine tetrahydrochloride (DAB) in the presence of 0.03% cobalt chloride, 0.03% nickel ammonium sulfate and 0.01% H_2O_2 and mounted on gelatin-coated glass slides. No tissue immunolabelling was detected when the primary antibody was incubated with 25 μg/ml of antigenic peptide or when the primary antibody was omitted.

Immunofluorescence of rat brain sections.—The procedure has been described elsewhere (Fekete et al., 2015; Fekete et al., 2017; X. Li, Serwanski, Miralles, Nagata, & De Blas, 2009; Y. Li et al., 2010). Briefly, free-floating brain sections, prepared as described above from P35 SD rats, were incubated with 5% normal goat serum (NGS)/0.3% Triton X-100/0.12M PB for 1 hour at RT, followed by incubation for 2 days at 4°C in a mixture of primary antibodies raised in different species in 2%NGS/0.3% Triton X-100 in 0.12M PB at 4°C. Sections were washed with PB and incubated in a mixture of fluorophore conjugated secondary antibodies in 2%NGS/0.3%Triton in 0.12M PB for 1 hour at RT. Sections were then washed again and mounted onto gelatin coated glass slides with Prolong Gold antifade mounting solution and imaged with a laser scanning confocal microscope.

In utero* electroporation.—In utero* electroporation was performed as previously described (Bai et al., 2003; F. Chen & LoTurco, 2012; Fekete et al., 2015; Frank et al., 2005; Y. Li et al., 2010; Ramos, Bai, & LoTurco, 2006). Briefly, pregnant Wistar rats (14 days of gestation) were deeply anesthetized as described above and laparotomy was performed. The uterine horns were pulled out and 1–3 μl of a sterile mixture of 0.5 μg/μl of pLZRS-CA-gapEGFP plasmid (gift from Drs. A. Okada and S. K. McConnell, Stanford University, Stanford, CA) and Fast Green (2 mg/ml; Sigma, St. Louis) was microinjected by pressure with a Picospritzer II (General Valve, Fairfield, NJ) through the uterine wall into a single lateral ventricle of each embryo (male and female) with a sterile pulled glass microelectrode (Drummond Scientific, Broomall, PA). Electroporation was accomplished with a BTX 8300-pulse generator (BTX Harvard Apparatus, Holliston, MA) and sterile BTX tweezertrodes applied to the embryo's head. Electroporation was carried out by a brief (1–2 msec) discharge of a 500-μF capacitor charged to 50–100 V. After electroporation, the uterus was returned to the abdominal cavity, and the incision was closed by sewing it up with sterile surgical suture. Metacam analgesic was administered daily at dosage of 1 mg/kg for 2 days following surgery. The pups were sacrificed at 35 days after birth.

Image acquisition, analysis and quantification.—Immunofluorescence images of cells in culture were collected with a Nikon Plan Apo 60×/1.40 oil immersion objective, in an Eclipse T300 microscope (Nikon Instruments) with an Andor Zyla 4.2 USB3 Digital camera (Oxford Instruments) driven by NIS Elements acquisition software (Nikon Instruments, RRID: SCR_014329). Confocal images of brain sections were acquired using an A1R laser scanning confocal microscope (Nikon Instruments) with a Plan Apo VC 60×/1.4 oil objective and a pinhole set at 1 Airy unit. Images were collected with NIS Elements acquisition software (Nikon Instruments, RRID: SCR_014329). The two- or three-color fluorescence images to be compared were merged for color co-localization in Photoshop CS5 (Adobe, San Jose, CA) and puncta manually counted. A Pcdh-γC4 puncta was considered co-localizing with another puncta or structure when 60–100% of the surface of the Pcdh-γC4 puncta overlapped with the puncta in another fluorescence channel. A Pcdh-γC4 puncta was considered to be adjacent to, or at the periphery of VGLUT1or VGAT puncta, when the edges of the puncta were 0–0.2 μm distant. All confocal microscope images presented in this study are from single optical sections. Statistical analysis was performed with InStat 3 (GraphPad, San Diego, CA, RRID: nlx_156835). Values are given as mean ± standard error of the mean (SEM).

RESULTS

Generation, validation and characterization of anti-Pcdh-γC4 antibody

A novel anti-Pcdh-γC4 antibody was made in rabbit to a unique synthetic peptide localized at the variable extracellular domain of Pcdh-γC4. Identical epitope amino acid sequence is present in rat, mouse and human Pcdh-γC4. The antibody was affinity-purified on immobilized peptide antigen.

To demonstrate specificity of the Ab for Pcdh-γC4 and not for the other Pcdh-γCs also missing in the TCKO (Pcdh-γC3 and Pcdh-γC5), we showed that the Ab gave very strong

immunofluorescence in HEK293 cells transfected with Pcdh-γC4-mCherry compared to the background immunofluorescence shown by non-transfected or cells transfected with mCherry, Pcdh-γC5-EGFP, cMyc-Pcdh-γC5 or Pcdh-γC3-EGFP (Fig. 1). These results indicate that the antibody specifically reacts with Pcdh-γC4 but not with the two closest relatives of the Pcdh-γC family (Pcdh-γC3 and Pcdh-γC5).

Database search of the antigen peptide DHAPRFPRQQLDLE revealed sequence homology with Pcdh8 (also called ARCADLIN and PAPC). The homologous sequence in Pcdh8 is DHAPRFPRAQIPVE corresponding to amino acids 130–139. Nevertheless, our anti-Pcdh-γC4 did not recognize overexpressed Pcdh8 in HEK293 cells (Fig. 2). A commercial Ms mAb to anti-Pcdh8 did not recognized HEK293 cells transfected with Pcdh-γC4-mCherry (Fig 2). In rat brain, triple-label immunofluorescence experiments show that Rb anti-Pcdh-γC4 and Ms anti-Pcdh8 show different labeling patterns (Fig. 3). While anti-Pcdh-γC4 labeling was frequently apposed to, but not co-localizing with, pre- or postsynaptic markers, anti-Pcdh8 labeling was frequently synaptic. Others have reported that Pcdh8 concentrates at excitatory synapses in cultured HP neurons (Keeler, Molumby, et al., 2015; Light & Jontes, 2017; Yamagata et al., 1999; Yasuda et al., 2007).

Additional demonstration of the specificity of the anti-Pcdh-γC4 Ab, shown below, includes: i) in cultured rat hippocampal neurons, anti-Pcdh-γC4 labelled puncta that were also co-labeled with a pan-Pcdh-γ mAb; ii) similar puncta were present in cultured hippocampal neurons from wild type and heterozygous mice but they were absent in the homozygous TCKO mice; iii) in rat and mouse brain immunoblots, the anti-Pcdh-γC4 Ab recognized a 120kDa protein, which was blocked by the antigenic peptide and was absent in the TCKO mouse; iv) the expression of the Pcdh-γC4 protein during brain development matched that of the Pcdh-γC4 mRNA; v) in immunocytochemistry of adult rat brain, the regional expression pattern of the Pcdh-γC4 protein revealed with the anti-Pcdh-γC4 Ab matched that of the Pcdh-γC4 mRNA expression (Allen Brain Atlas http://mouse.brain-map.org/experiment/show/70784958) and vi) the antigenic peptide blocked the reaction of the Pcdh-γC4 Ab with brain tissue.

Immunoblots from adult rat forebrain membranes showed three main protein bands corresponding to ~120, 55 and 40 kD (Fig. 4a). The immunoreactivity of the three proteins was displaced by peptide antigen (20 μg/ml, strip P). The 120,000 Mr protein band corresponds to the mobility of the glycosylated Pcdh-γC4 (Frank et al., 2005). The 120 kD protein was present in immunoblots of mouse and rat brain homogenates of various ages (Fig. 4b–d). In mouse, it was present in the P0 wild type (WT) but absent in the homozygous (HZ) P0 TCKO littermates (Fig. 4b and d). The TCKO mouse does not survive beyond P0. The 55 and 40 kD protein bands were still present in the TCKO, indicating that these proteins were not derived from Pcdh-γC4.

During development of the rat brain, the 120 kD Pcdh-γC4 were already expressed at E18 (earliest time tested, Fig. 4b). The levels of expression were relatively high at E18, P0, P7 and P14, then decreasing at P21 and maintaining similar lower level of expression at P30, P45 and P90 (Fig. 4d). Although decreased, compared to earlier postnatal age (P0–P21), there is a significant expression of Pcdh-γC4 protein in the adult rat brain.

Pcdh-γC4 is highly enriched in rat brain membranes (P37) over the brain homogenates of comparable age (P30 and P45), as shown in immunoblots (Fig. 4c). This enrichment in membranes is expected for a cell-adhesion membrane protein.

Rat hippocampal neurons express Pcdh-γC4 at different levels.

In 21 DIV rat HP neuronal cultures, the Rb anti-Pcdh-γC4 reveals the presence of Pcdh-γC4 puncta in the soma and dendrites of pyramidal neurons and GABAergic interneurons (Fig. 5). Double-label immunofluorescence showed that 95±2% of Rb anti-Pcdh-γC4 puncta (620 puncta, n=4 neurons) were also labeled with the mouse anti-pan-Pcdh-γ antibody (Fig. 5a–c), validating the immunofluorescence signal obtained with the Rb anti-Pcdh-γC4 antibody. Validation was also done with the TCKO mouse described below.

The rat hippocampal glutamatergic pyramidal neurons show a large variability in the levels of expression of Pcdh-γC4. Some (39%, n=25, out of 64 pyramidal neurons) show large Pcdh-γC4 puncta (≥0.25 μm^2), some of these puncta being very large (≥3 μm^2) and of high fluorescence intensity, as shown by the pyramidal neuron in Fig. 5d (which is also GAD-). Other pyramidal neurons (61%, n=39, out of 64 pyramidal neurons) show considerably fewer and smaller (<0.25 μm^2) puncta with lower fluorescence intensity (Fig. 5e). Pyramidal neurons are identified by their large size, shape and absence of GAD expression.

The large majority of interneurons (85%, n=29, out of 34 interneurons), identified by the expression of GAD in their somas (Fig. 5f–i), have very large (as large as 5–20 μm^2, arrows) Pcdh-γC4 puncta of very high fluorescence intensity (Fig. 5d–f). A small population of interneurons (15%, n=5, out of 34 interneurons) had fewer and smaller (<0.25 μm^2) Pcdh-γC4 puncta (Fig. 5i). As a general rule, interneurons had more and larger puncta of higher fluorescence intensity than pyramidal neurons. The largest puncta in interneurons (Fig. 5f–h, arrows) are larger than the largest puncta in pyramidal neurons (Fig. 5a and d). In both pyramidal and interneurons, the largest puncta tend to be localized in the somas and proximal dendrites, but large puncta are also present in the distal dendrites of some neurons (Fig. 5d, f and g).

The results show that I) most, if not all, HP neurons express Pcdh-γC4; II) there is a large range of expression of Pcdh-γC4 among various pyramidal cells and among various interneurons and III) HP interneurons express higher levels of Pcdh-γC4 than pyramidal neurons.

The relative levels of Pcdh-γC4 protein expression in HP pyramidal neurons and interneurons are consistent with results using an antibody that recognizes all Pcdh-γs (Phillips et al., 2003). Nevertheless, there is evidence showing that not all members of the Pcdh-γ family have similar relative levels of expression in HP neurons. For instance, Pcdh-γC5 is highly expressed in pyramidal neurons (Y. Li et al., 2010) while Pcdh-γC4 is highly expressed in interneurons.

When live neurons were surface-labeled with anti-Pcdh-γC4, the immunofluorescent puncta were highly decreased in number and intensity (Fig. 5j, arrowheads) compared with those observed in fixed and Triton X-100 permeabilized neurons (Fig. 5k). Arrows point to large

Pcdh-γC4 puncta present in the somas. These results are consistent with those of another group who has shown, by using a different antibody (a Rb pan-Pcdh-γ), that these puncta observed in cultured neurons largely correspond to trafficking organelles including endoplasmic reticulum and various types of endosomes (Fernandez-Monreal, Kang, & Phillips, 2009; Fernandez-Monreal et al., 2010).

The predominant localization of Pcdh-γC4 and other Pcdh-γs in intracellular organelles in cultured neurons, and in the absence of contacting astrocytes, is consistent with the immuno-EM studies in brain tissue. In a study using the aforementioned Rb pan Pcdh-γ antibody to a cytoplasmic epitope, the authors (Fernandez-Monreal et al., 2010) showed preferential intracellular organelle labeling of Pcdh-γs. The presence of Pcdh-γC4 in both the cell surface and intracellular organelles of cultured neurons is consistent with another immuno-EM study with a Rb antibody to a unique extracellular epitope Pcdh-γC5, which showed strong intracellular organelle labeling but also significant amount of labeling of the plasma membrane (Y. Li et al., 2010).

Below we are studying the expression of Pcdh-γC4 in brain by laser confocal microscopy immunofluorescence, which requires the use of Triton X-100 for membrane permeabilization and antibody penetration.

Pcdh-γC4 puncta are present in mouse hippocampal neurons from wild type but not Pcdh-γC deficient mice.

The TCKO mice die shortly after birth at P0. However, healthy HP neurons from E18 mutant and wild type mouse embryos can be maintained in culture for at least 21DIV (Y. Li et al., 2012), as for rat HP neuronal cultures.

Neurons from 21 DIV HP cultures of WT mouse showed Pcdh-γC4 puncta in soma and dendrites (Fig. 6a and d), similar to those observed in rat neurons (Fig. 5). Also similar to rat, there is a large variability in the levels of Pcdh-γC4 expression in mouse HP neurons. In general, the Pcdh-γC4 puncta in HP mouse neurons (seldom larger than 2 μm^2) did not reach the very large size observed in some HP rat neurons.

In contrast, none of the cultured 21 DIV HP neurons from the TCKO littermate homozygous showed Pcdh-γC4 puncta. They showed just a diffuse and low background fluorescence (Fig. 6 g and J). These results also validate the Rb anti-Pcdh-γC4 antibody for immunofluorescence.

In HP cultures of the WT mouse, the large majority of neurons also expressed Pcdh-γA as shown by the presence of puncta with a pan-Pcdh-γA antibody (Fig. 6b and e). In individual neurons, a large proportion of the Pcdh-γA puncta (58±4%, of 426 puncta, n=4 neurons,) co-localized with Pcdh-γC4 puncta and 54±3% of Pcdh-γC4 puncta (of 449 puncta, n=4 neurons) co-localized with Pcdh-γA puncta (Fig. 6b, c, e and f, arrows). Filled arrowheads point to some Pcdh-γC4 puncta that do not co-localize with Pcdh-γA puncta and empty arrowheads point to some Pcdh-γA puncta that do not co-localize with Pcdh-γC4 puncta. These results suggest that within the same neuron of the WT mouse, the composition of Pcdh-γ puncta is heterogeneous.

The TCKO mutant neurons, which had no Pcdh-γC4 puncta (Fig. 6g and j), did have Pcdh-γA puncta, as revealed by the pan-Pcdh-γA antibody (Fig. 6h and k). Thus, expression and clustering of Pcdh-γCs is not essential for the clustering of Pcdh-γAs. These results agree with mRNA expression studies in the TCKO mouse brain, which show no significant changes in the expression of Pcdh-γAs in the mutants compared with the WT (W. V. Chen et al., 2012).

HP neurons of the TCKO mouse are not deficient in their ability to form glutamatergic synaptic contacts, as determined by immunofluorescence with VGLUT1 and PSD-95 antibodies (Fig. 7), nor in their ability to form GABAergic synaptic contacts (Y. Li et al., 2012).

Some Pcdh-γC4 puncta localize at contact points between axons and neurons, near but not on synapses.

Studying rat hippocampal cultures, we found that a subset of Pcdh-γC4 puncta (green) were present at contact points between GABAergic axons (blue) and neuronal dendrites (Fig. 8a–d). Fig. 8a and c show a pyramidal neuron at the left side, with small Pcdh-γC4 puncta, and dendrites from GAD+ interneuron at the right side of the panel with larger Pcdh-γC4 puncta, both contacted by thin GAD+ GABAergic axons. Empty arrowheads indicate dendritic Pcdh-γC4 puncta lined up with axons, while filled arrowheads show puncta associated with GAD+ boutons. Fig. 8b and d show another example of a GABAergic axon contacting a dendrite from a GAD+ neuron. These results are consistent with another study with an antibody that recognizes all Pcdh-γs in HP cultures of an earlier age (8DIV) (Fernandez-Monreal et al, 2009).

We investigated whether the Pcdh-γC4 puncta associated to contacts between axons and neurons were at synapses (Fig. 8e–g). In cultured neurons 47±3% of GABAergic synapses (gephyrin+ and GAD+) had Pcdh-γC4 puncta associated with them (249 synapses, n=4 neurons). The majority of these Pcdh-γC4 puncta (arrowheads) were near the synapse but not at the synapse (*i.e.* they were at the periphery of, or adjacent to GAD+ boutons but they did not co-localize with gephyrin clusters). Moreover, the large majority of gephyrin clusters (synaptic or non-synaptic) did not co-localize with Pcdh-γC4; only a few (9±3%, 648 clusters, n=4 neurons) gephyrin clusters co-localized with Pcdh-γC4 (Fig. 8g, arrow).

We also studied the relationship of Pcdh-γC4 puncta with glutamatergic synapses. Fig. 8h–j shows triple-label immunofluorescence with Pcdh-γC4 (green), VGLUT1 (blue) and PSD-95 (magenta). Although 28±4% of the glutamatergic synapses (PSD-95+ and VGLUT1+, 811 synapses, n=3 neurons) had associated Pcdh-γC4 puncta (Fig. 8h), only 12±4% of the VGLUT1 puncta (569, n=3 neurons) (Fig. 8i) and 11±3% of the PSD-95 clusters (328, n=3 neurons) (Fig. 8j) co-localized with Pcdh-γC4 puncta. More frequently, the Pcdh-γC4 puncta were adjacent to, or at the periphery of VGLUT1 puncta or PSD-95 clusters rather than co-localizing with them.

The results indicate that I) the large majority of Pcdh-γC4 puncta are not associated with synapses and II) that the majority of Pcdh-γC4 puncta that are associated with GABAergic or glutamatergic synapses are near but not co-localizing with synaptic contacts. Some of the

Pcdh-γC4 puncta, even if not localized at the plasma membrane but rather in intracellular organelles, could be involved in the regulation of adhesion between axons and contacting dendrites and somas.

Pcdh-γC4 is also expressed by astrocytes

We prepared astrocyte cultures and identified them by the expression of GFAP. Double immunofluorescence experiments show that the GFAP (magenta)-expressing astrocytes also expressed Pcdh-γC4 (green), which formed puncta that concentrate in the cell body (Fig. 9a, b, d and f). Pcdh-γC4 immunofluorescence was also present at the plasma membrane (Fig. 9e) and astrocyte processes (Fig. 9c and g). Thus, Pcdh-γC4 is expressed in cultured neurons and astrocytes forming puncta. Many of the puncta likely correspond to labeling of intracellular trafficking organelles, including endoplasmic reticulum and endosomes, as shown in cultured neurons and in brain extracts containing neurons and astrocytes (Fernandez-Monreal et al., 2009; Fernandez-Monreal et al., 2010; Phillips, LaMassa, & Nie, 2017).

Rat brain ICC with anti-Pcdh-γC4.

We have studied the expression of Pcdh-γC4 in the rat brain by both ICC and immunofluorescence. Light microscopy immunocytochemistry of young adults (P35) shows (Fig. 10a) that the highest expression of Pcdh-γC4 occurs in the olfactory bulb (OB, particularly in the olfactory glomeruli, and less in the external plexiform layer), cerebellum (CB), superior colliculus (SC), dentate gyrus (DG), hippocampus (HP), substantia nigra (SN) and pontine nuclei (PN), with lower expression in the cerebral cortex (CC) and corpus striatum (St). No immunolabelling was obtained by incubating the antibody with antigenic peptide (20–100 μg/ml) or by omitting the primary antibody.

The distribution of anti-Pcdh-γC4 immunoreactivity in the rat brain is consistent with the expression of the Pcdh-γC4 mRNA in the adult mouse, as shown by *in situ* hybridization (ISH) in the Allen Brain Atlas (http://mouse.brain-map.org/experiment/show/70784958).

The ISH data shows the highest Pcdh-γC4 mRNA expression in olfactory bulb (periglomerular cells, mitral cell layer and granule cell layer), cerebellum (Purkinje cell layer and granule layer), dentate gyrus and hippocampus. It also shows lower Pcdh-γC4 mRNA expression in the cerebral cortex and very low expression in the corpus striatum.

In the HP (Fig. 10b and c), the immunoreactivity was highest in the stratum pyramidale (SP) and hilus (HL), showing a punctate appearance. In the DG (Fig. 10e and f), the immunoreaction was highest in the boundary between the granule cell layer (GR) and the plexiform layer (PL), also showing granular appearance. In CB (Fig. 10h–j), the granule cell layer (GR) showed the highest immunoreaction; particularly in the boundary with the Purkinje cell layer (PK) where the immunoreaction also had a punctate aspect. Concentration of these puncta appeared in the GR layer (Fig. 10i and j, white arrowheads), sometimes surrounding blood vessels (black arrow) and also in the boundary between PK and the GR layers (black arrowheads). In the OB (Fig. 10d), high immunoreaction occurred in the olfactory glomeruli (OG, white asterisks), particularly surrounding the glomeruli (white arrowheads). Considerably less immunoreaction was observed in the cerebral cortex

(Fig. 10g). It is worth noting that the areas where the Pcdh-γC4 immunoreactivity was highest coincided with boundaries between anatomically defined layers or structures (OG borders, boundary between GR and PL layers in DG, or between PK and GR layers in cerebellum, or between blood vessels and neuropil). Although in the adult brain the distribution of Pcdh-γC4 immunoreactivity shown above is quite different from that of Pcdh-γC5, which we have reported elsewhere (Y. Li et al., 2012), in both cases, the immunoreaction presents a similar punctate appearance.

Rat brain immunofluorescence with anti-Pcdh-γC4.

We performed immunofluorescence of P35 rat brain sections with the Rb anti-Pcdh-γC4. There was very good agreement with the ICC results regarding the relative expression of Pcdh-γC4 in various brain regions, including the high level of immunofluorescence in the olfactory bulb (Fig. 11a–f, magenta), the granule layer of cerebellum (Fig. 11g and h, magenta and Fig. 12a, green), and the dentate gyrus, particularly in the boundary between plexiform layer and granule layer (Fig. 12b, green). Pcdh-γC4 immunofluorescence was manifested in the form of bright puncta in the neuropil and around the neuronal somas.

Olfactory Bulb.—The olfactory bulb showed the highest level of Pcdh-γC4 immunofluorescence in rat brain (Fig. 11a–f, magenta). The olfactory glomeruli (OG) had very large periglomerular Pcdh-γC4 puncta as well as smaller puncta inside the glomeruli (Fig. 11a, c and e, magenta). VGLUT1 immunofluorescence (blue) revealed the presence of glutamatergic presynaptic contacts at the edge of, and deep inside the OGs. Although many Pcdh-γC4 puncta were not associated with VGLUT1 puncta, the large majority of the latter had associated Pcdh-γC4 puncta deep inside the OG (Fig. 11c arrow) and at the edge of the OG (Fig. 11e arrowheads). The olfactory glomeruli could be easily identified with diffuse PSD-95 immunofluorescence, which was absent from the periglomerular strip. (Fig. 11a, green).

Fig. 11b and d show immunofluorescence at the OB granule cell layer. There is frequent grouping of granule cell somas into cell aggregates (i.e. cell aggregates 1–4). The Pcdh-γC4 puncta and VGLUT1 puncta are localized between the aggregates, but seldom inside these aggregates. It has been shown that the granule cells of an aggregate are electrically coupled to each other (Reyher et al., 1991). Fig. 11f is from the external plexiform layer, which also shows postsynaptic PSD-95 immunofluorescence (green). The Pcdh-γC4 puncta are near but do not co-localize with glutamatergic synapses. They are frequently adjacent to VGLUT1 puncta. In the external plexiform layer 77.9±2% (of 322 puncta, n=3 images) of the VGLUT1 puncta had one or more Pcdh-γC4 puncta at the periphery. This is not by chance. By rotating one of the two overlaid images180 degrees, the values drop to 20.6±1% (of 322 puncta, n=3 images). Note the larger size of the Pcdh-γC4 puncta in OG (Fig. 11e) compared to the size of the Pcdh-γC4 puncta in the external plexiform layer of the OB (Fig. 11f).

Cerebellum.—Double-label immunofluorescence with anti-VGLUT1 and anti-Pcdh-γC4 revealed that Pcdh-γC4 puncta were more abundant in the granule cell layer (GR) than in the molecular layer (ML) (Fig. 11g and h). In GR, Pcdh-γC4 puncta were particularly bright

and large at the boundary between GR and Purkinje cell (PK) layer (Fig. 11g, arrow). In GR, Pcdh-γC4 puncta were concentrating in the periphery of the VGLUT1-labeled synaptic glomeruli, particularly between the glomeruli and granule cells (Fig. 11h, arrowheads). Granule cells frequently formed rows (Fig. 11h asterisks). Pcdh-γC4 puncta were largely absent from the contacts between granule cells within a row. Pcdh-γC4 puncta were associated with the surface of PK somas (Fig. 11g, arrow). In the molecular layer, Pcdh-γC4 puncta frequently had a radial orientation (Fig. 11g, arrowheads).

We have also studied the relationship between Pcdh-γC4 puncta and GABAergic synapses. In the cerebellum, the Pcdh-γC4 puncta (green) were often associated with VGAT-labeled (blue) presynaptic terminals present at the periphery of the synaptic glomeruli (Fig. 12a, crossed arrows) and the soma of PK cells (Fig. 12a, arrowheads). Moreover, VGAT immunofluorescence (blue) revealed the pinceaux of the basket cell axons synapsing onto the axon initial segment of PK cells (i.e. PK cell 2 and partially in PK cell 1 in Fig. 12a). These pinceaux had a high number of associated Pcdh-γC4 puncta (Fig. 12a, arrows).

Cerebral cortex.—Pcdh-γC4 puncta (green) were associated with the surface of the neuronal somas and at the neuropil (Fig. 12c–h). Numbers 3–7 identify the soma of some neurons. There were also Pcdh-γC4 puncta associated with the wall of blood vessels (Fig. 12c, # symbol). A subset of Pcdh-γC4 puncta were associated with VGAT puncta (blue), both at the surface of the neuronal soma and at the neuropil, although the large majority of the Pcdh-γC4 puncta were not associated with VGAT. When there was association, Pcdh-γC4 puncta were often localized at the edges of VGAT puncta, as can be observed at high magnification (Fig. 12d, e, g and h, arrowheads). In fact, 41.8±3% (of 254 puncta, n=3 images) of VGAT puncta had Pcdh-γC4 puncta at the periphery. When one of the two overlaid images was rotated 180 degrees, the values dropped to 18.7±1% (of 254 puncta, n=3 images). The results suggest a frequent perisynaptic localization of the associated Pcdh-γC4 puncta. The Pcdh-γC4 puncta did not co-localize with gephyrin clusters (magenta, Fig. 12i and j), although they frequently were apposed to them (Fig. 12i and j, arrowheads).

We also performed double-label immunofluorescence of Pcdh-γC4 with the astrocyte marker S-100β. Fig. 12k–m shows that in the cerebral cortex, Pcdh-γC4 puncta (magenta) were frequently associated with the surface of both the astrocyte (green) cell bodies and processes (Fig. 12k–m, arrowheads). Prominent and frequently large Pcdh-γC4 puncta were found on astrocyte processes associated with blood vessels (Fig. 12k, # symbol), which agrees with the granular aspect of the reaction on the wall of the capillaries observed by ICC (*i.e.* Fig. 10j, arrow).

Pcdh-γC4 forms puncta frequently associated with contact points between neurons and astrocytes.

Figs. 11 and 12 indicate that Pcdh-γC4 puncta are frequently associated with the surface of neuronal somas and apposed to synapses (both glutamatergic and GABAergic synapses) in various brain regions. Fig. 12k–m indicates that Pcdh-γC4 puncta are frequently associated with the surface of astrocytes in the cerebral cortex. We have investigated whether Pcdh-γC4 puncta associate with the contact points between astrocytes and neurons. For this purpose,

we *in utero* electroporated rats with EGFP, aiming to EGFP-label a limited number of cortical neurons. This allowed us to visualize individual neurons and processes, which cannot easily be accomplished by using an antibody to a neuronal marker that labels most neurons. Fig. 13 shows that in the cerebral cortex of the P35 IUEP rat, many individual Pcdh-γC4 puncta (magenta) localize with both astrocyte processes revealed with anti-S100β (blue) and transfected neurons (soma or dendrites, green) as shown by arrowheads. Thus, 89% of all Pcdh-γC4 puncta (672 puncta on 11 transfected neurons, including somas and 15 dendrites, from 3 different images) localized on or in contact with the dendrites and soma of EGFP-fluorescent neurons also co-localized with astrocyte processes, revealed with anti-S100β labeling. After rotating one of the overlaid images 180 degrees (Pcdh-γC4 red), the co-localization values dropped to 29% (of 315 puncta on 11 transfected neurons, including somas and 15 dendrites, from 3 different images co-localized with astrocyte processes). The frequent association of individual Pcdh-γC4 puncta with both neurons and astrocyte processes strongly suggest an association of many Pcdh-γC4 puncta with neurons and astrocyte contacts. This interpretation is consistent with: I) the observed expression of Pcdh-γC4 in neurons and astrocytes; II) the proposed Pcdh-γ trans-homophilic interactions and III) the enrichment of the120 kD Pcdh-γC4 protein band in immunoblots of brain membranes compared to the homogenates (Fig. 4c and d).

We have also investigated in other brain regions the relationship between Pcdh-γC4 puncta and astrocyte processes. In the OB (Fig. 14a–c), Pcdh-γC4 puncta (green) are frequently associated with the interface (arrowheads) between astrocytes (blue) and the somas (ghosts) of periglomerular neurons (asterisks) surrounding an olfactory glomerulus (GL), as shown in Fig. 14a. There are also Pcdh-γC4 puncta in the glomerulus (GL) associated with astroglial processes (from periglomerular astroglial cells). In the granule layer of the OB (Fig. 14b), Pcdh-γC4 puncta are present throughout the layer, associated with astrocyte somas and processes, frequently apposed to synapses (arrowheads) as shown by VGAT immunofluorescence (magenta). Pcdh-γC4 puncta are largely absent from granule cell to granule cell contacts, in the aforementioned granule cell aggregates (Fig. 14b asterisks). The association with astrocyte processes and the frequent apposition of the Pcdh-γC4 puncta to synapses is also found in the external plexiform layer of the OB (Fig. 14c, arrowheads).

In the cerebellum (Fig. 14d–g), Pcdh-γC4 puncta (green) are associated with the surface of Bergmann glia cell bodies (blue), which localized at PK (Fig. 14d, arrow) and Bergmann glia processes, which are located in ML (Fig. 14d, arrowheads). Fig. 14f shows the association between Pcdh-γC4 puncta with Bergmann glia radial fibers (arrowheads) and the network of fine glial processes between the thicker fibers. Some of these puncta are apposed to VGAT terminals. Fig. 14e shows the wrapping of a Purkinje cell soma by Bergmann glia (blue) and the presence of Pcdh-γC4 puncta between the two cell types (arrowheads). Fig. 14e also shows that Pcdh-γC4 puncta (green) associated with the pinceaux (VGAT+, magenta, asterisk) and glial cell processes (blue). In the granule cell layer (Fig. 14g), the Pcdh-γC4 puncta are localized at the interface (likely contacts) between astrocyte processes and the somas of granule cells (arrowheads) and also at the boundary between the synaptic glomeruli (rich in GABAergic contacts, magenta) and the astrocyte processes wrapping them (arrows).

DISCUSSION

Much of our knowledge on the function of clustered Pcdhs in the brain is derived from studying mouse mutants in which a whole family or subfamily of clustered Pcdhs have been deleted (or tagged for tracing). Nevertheless, considerably less is known on the functional roles of individual Pcdhs within a family or subfamily. The GKO mouse, in which the whole Pcdh-γ family has been deleted, and the TCKO mouse, in which only the three the C-type members of the Pcdh-γ family are missing, show similar phenotypes such as perinatal death at P0 and interneuron losses in spinal cord and retina (W. V. Chen et al., 2012). These results indicate that one or more of the three C-type Pcdh-γs are essential for postnatal animal survival and prevention of apoptosis in a subset of interneurons. It has not yet been determined which of the three C-type Pcdh-γs is/are essential for neuronal and mouse survival, since no individual C-type Pcdh-γ mouse KOs are available. The reason why the C-type Pcdh-γs are essential for these functions, but not the other Pcdh-γs or the members of the Pcdh-β or Pcdh-α families, is not understood. One possibility might be derived from the reported constitutive expression of the C-type Pcdh-γs in most neurons *vs.* the stochastic (non-essential) expression of the other members of the Pcdh-γs family (Esumi et al., 2005; Frank et al., 2005; Hirano et al., 2012; Hirayama & Yagi, 2017; Kaneko et al., 2006; Mountoufaris et al., 2017). Nevertheless, some neurons, like olfactory sensory neurons (OSN), do not express C-type Pcdh-γs (Mountoufaris et al., 2017).

In an effort to elucidate the role of individual C-type Pcdh-γs, we have previously studied the spatial-temporal and cellular expression of Pcdh-γC5 in the rat brain, using an antibody developed in our laboratory (Y. Li et al., 2010). These studies showed that Pcdh-γC5 is involved in i) the regulation of the surface expression of $GABA_A$Rs and ii) in the stabilization and maintenance of a subset of GABAergic synapses (Y. Li et al., 2012). More recently, it has been proposed that during Alzheimer's disease there is aberrant Pcdh-γC5 expression and GABAergic synaptic dysfunction (Y. Li et al., 2017).

In the present communication, we have studied Pcdh-γC4 protein expression in the rat brain with a novel anti-Pcdh-γC4 antibody, which we have developed in our laboratory. To the best our knowledge, this is the first report of the Pcdh-γC4 protein expression in brain and brain cells. The expression of Pcdh-γC4 mRNA in adult P56 mouse brain has been revealed by *in situ* hybridization (Allen Brain Atlas http://mouse.brain-map.org/experiment/show/70784958). Northern blot analysis of the developmental expression of Pcdh-γC4 mRNA in the mouse brain has also been reported (Frank et al., 2005). Our Pcdh-γC4 protein data in rat brain agrees very well with the reported regional mRNA expression in mouse. Both reveal the highest levels of expression of Pcdh-γC4 in olfactory bulb, cerebellum and dentate gyrus of HP. Regarding developmental expression, the highest level of Pcdh-γC4 protein expression occurs in embryos and the first two weeks after birth. Although downregulated, there is a significant level of Pcdh-γC4 protein expression in adult rat brain, which agrees with Pcdh-γC4 mRNA developmental studies in mouse (Frank et al., 2005). We have also found that HP interneurons have larger and brighter Pcdh-γC4 puncta than pyramidal neurons, and that Pcdh-γC4 is also expressed in astrocytes. These results are also in agreement with recent single-cell RNA-seq data in the visual cortex of P56 adult mouse

https://portals.broadinstitute.org/single_cell/study/a-transcriptomic-taxonomy-of-adult-mouse-visual-cortex-visp

Unique properties of Pcdh-γC4 with respect to the other two Pcdh-γCs

The two specific Abs revealed clear differences between Pcdh-γC4 and Pcdh-γC5. We have previously shown (Y. Li et al., 2012) that Pcdh-γC5 directly cis-interacts with the γ2 subunit of the $GABA_A$Rs (via their cytoplasmic domain of Pcdh-γC5 and the large cytoplasmic loop of the γ2 subunit). Moreover, anti-Pcdh-γC5 co-precipitated 23% of solubilized $GABA_A$Rs from brain membranes. In contrast, no $GABA_A$Rs could be co-precipitated with anti-Pcdh-γC4. This result is consistent with Pcdh-γC4 lacking the critical residues which are found in Pcdh-γC5 to be responsible for the interaction with $GABA_A$Rs (Y. Li et al., 2012).

Another difference is that in rat and mouse, Pcdh-γC5 protein is not expressed until after the second postnatal week (Y. Li et al., 2012), while Pcdh-γC4 protein is expressed at highest levels in the embryo and during the first two postnatal weeks, decreasing its expression in the adult (Fig 4). Pcdh-γC3 mRNA is expressed in the embryo and the adult brain (Frank et al., 2005). The relative expression of Pcdh-γC3, Pcdh-γC4 and Pcdh-γC5 mRNA varies not only during development but also through various brain regions in the adult mouse (http://mouse.brain-map.org), indicating distinct roles for each Pcdh-γC.

In terms of protein, comparison of the Pcdh-γC4 immunofluorescence data of this study with that of Pcdh-γC5 (Y. Li et al., 2010), shows that there are differences in the relative expression levels of Pcdh-γC4 and Pcdh-γC5 in various brain regions. Thus, corpus striatum and hippocampal CA1 show high Pcdh-γC5 but low Pcdh-γC4 levels of protein expression. In cerebellum, Pcdh-γC4 is preferentially expressed in the granule layer while Pcdh-γC5 expression is higher in the molecular layer. Thus, even though Pcdh-γC4 and Pcdh-γC5 are thought to be constitutively expressed in most neurons, there is a large variability in the relative levels of expression across brain regions and cell types. Another difference is the higher relative expression of Pcdh-γC4 in GABAergic interneurons and of Pcdh-γC5 in pyramidal neurons of the HP.

Another difference is that Pcdh-γC5 (Y. Li et al., 2012; Thu et al., 2014) or Pcdh-γC3 (Frank et al., 2005; Schreiner & Weiner, 2010; Thu et al., 2014), when expressed alone, induce trans-homophilic cell adhesion. However, Pcdh-γC4 does not (Fernandez-Monreal et al., 2009; Thu et al., 2014), apparently because in host cells, Pcdh-γC4 by itself cannot translocate from internal stores to the cell surface (Fernandez-Monreal et al., 2009; Shonubi, Roman, & Phillips, 2015). Likewise, Pcdh-αs do not translocate to the cell surface by themselves (Thu et al., 2014). Nevertheless, Pcdh-γC4 and Pcdh-αs do translocate to the cell surface when they are co-expressed with other Pcdh-γs or Pcdh-βs, forming cis-heterodimers, which are thought to be the units for trans-homophilic Pcdh cell-adhesion (Brasch et al., 2019; Thu et al., 2014). Therefore, in neurons, which normally co-express multiple Pcdh-γs and Pcdh-βs (Frank et al., 2005; Hirano et al., 2012; Mountoufaris et al., 2017), Pcdh-γC4 is expected to form heterodimers with them and translocate to the cell surface. This notion is consistent with i) the enrichment of Pcdh-γC4 in brain membranes over homogenates (Fig 4) and ii) the Pcdh-γC4 immunofluorescence of rat brain sections, which shows that most of the labeling is associated with the cell surface of neurons and

astrocytes (Figs 12–14). Note that the term “association” does not imply that Pcdh-γC4 puncta correspond to molecules localized at the plasma membrane. They could also be cytoplasmic organelles localized near the plasma membrane of neurons and astrocytes.

Additional functional differences have been recently reported in that Pcdh-γC3 downregulates, Pcdh-γC4 has no effect and Pcdh-γC5 upregulates Wnt signaling, respectively (Mah, Houston, & Weiner, 2016).

Role of Pcdh-γC4 in synapses

In HP cultures, a subset of Pcdh-γC4 puncta were associated with synapses. Moreover, 47% of GABAergic synapses and 28% of glutamatergic synapses had associated Pcdh-γC4 puncta. However, the majority of Pcdh-γC4 puncta associated with synapses were not localized at the synaptic contacts themselves. Only 9% of gephyrin clusters and 11% of PSD-95 clusters co-localized with Pcdh-γC4 puncta. We and others have previously shown that other Pcdh-γs are associated with synapses but not exclusively (Blank, Triana-Baltzer, Richards, & Berg, 2004; Frank et al., 2005; Y. Li et al., 2010; Y. Li et al., 2012; Phillips et al., 2003; Wang et al., 2002).

We also found that cultured HP neurons from the TCKO mouse had many glutamatergic (Fig. 7) and GABAergic synapses (Y. Li et al., 2012), indicating that C-type Pcdh-γs are not essential for the formation or maintenance of excitatory or inhibitory synapses. Nevertheless, in the TCKO neuronal cultures there was a decreased number (20–25%) of GABAergic synapses (Y. Li et al., 2012), which could also be due to apoptosis of some interneurons resulting in decreased number of GABAergic axon making synapses (Y. Li et al., 2012). Therefore, although not essential, Pcdh-γs might still play a role in the normal development of synapses in these HP cultures. This notion is consistent with studies on the GKO mouse showing that Pcdh-γs play a role in the normal development of synapses in spinal cord and retina (Garrett & Weiner, 2009; Wang et al., 2002; Weiner et al., 2005). We have found that in the rat brain, Pcdh-γC4 puncta are frequently associated with neuron-astrocyte contacts and apposed to synapses, suggesting a synaptic supporting role, as discussed below.

Possible role of Pcdh-γC4 in preventing apoptosis of some interneurons.

Both GKO (Lefebvre et al., 2008; Prasad et al., 2008; Wang et al., 2002; Weiner et al., 2005) and TCKO mice (W. V. Chen et al., 2012) die at P0 and show similar loss of a subset of interneurons in spinal cord and retina (and also retinal ganglion cells) due to apoptosis, indicating that interneuron death results from the loss of the C-type Pcdh-γs. Apoptosis in the GKO mouse retina can occur in the absence of major synaptic defects (Lefebvre et al., 2008) while in the spinal cord, synapses can be lost in the absence of apoptosis (Weiner et al., 2005), suggesting that apoptosis and synaptic defects result from disruption of different signaling pathways mediated by Pcdh-γs. Nevertheless, some reductions in the number of synapses (not in the synaptic organization of the circuits) might also result from a reduced number of interneurons (Lefebvre et al., 2008).

Pcdh-γC5 is not expressed until after the second postnatal week, indicating that the deletion of Pcdh-γC5 in the TCKO plays no role in the phenotype of the TCKO mouse (perinatal animal death and apoptosis of a subset interneurons in spinal cord and retina). In contrast,

Pcdh-γC4 is expressed at highest levels in the embryo and during the first two postnatal weeks making the Pcdh-γC4 a strong candidate for preventing interneuron apoptosis and allowing perinatal survival. This notion is also supported by the high level of Pcdh-γC4 protein expression in interneurons. Pcdh-γC3, the third deleted C-type Pcdh in the TCKO mouse, is also a candidate for the phenotype, since Pcdh-γC3 mRNA is expressed in both the embryo and the adult brain (Frank et al., 2005).

Interestingly, the role of Pcdh-γ in neuronal survival in the spinal cord is not cell-autonomous (Prasad et al., 2008), although in the retina, neuronal survival also has a cell autonomous component (Lefebvre et al., 2008). In the spinal cord, Pcdh-γ-deficient interneurons can survive if surrounded by normal neurons and normal interneurons can undergo apoptosis if they are surrounded by Pcdh-γ-deficient motor neurons (Prasad et al., 2008). These results suggest that the role of Pcdh-γC in preventing apoptosis of these interneurons in the spinal cord might involve the release of trophic factors that require the expression of Pcdh-γCs (Prasad et al., 2008).

Role of Pcdh-γC4 in astrocytes.

It has been proposed that Pcdh-γs are involved in perisynaptic neuron-astrocyte interactions promoting synaptogenesis in the embryonic spinal cord (Garrett & Weiner, 2009). More recent studies show that Pcdh homophilic interactions between neurons and glia regulate dendritic arborization (Molumby et al., 2016). Nevertheless, the identification of the individual Pcdh-γ(s) involved in the perisynaptic and other neuron-glia contacts has not been addressed. We found that astrocytes express Pcdh-γC4, as do neurons. Moreover, in the brain, Pcdh-γC4 puncta frequently associate with contacts between neurons and astrocyte processes and are apposed to synapses. Robust Pcdh-γC4 puncta are also found at the contact point between astrocyte end-feet and the wall of capillaries, suggesting a recognition role between capillaries and astrocytes. We have previously shown that Pcdh-γC5 was also expressed in neurons and astrocytes forming puncta that concentrate at neuron-astrocyte contacts and at astrocyte end-feet (Y. Li et al., 2010). However, Pcdh-γC4 and Pcdh-γC5 are differentially expressed in various neuronal and glial cells and brain regions, as discussed above.

The presence of Pcdh-γC4 in astrocyte-neuron contacts is not essential for synapse formation. Fig. 7 shows that there are many excitatory and inhibitory synapses in HP cultures of the TCKO Pcdh-γC-null mouse (Y. Li et al., 2012). We and others have also found that neuronal cultures from Pcdh-γ-null GKO mouse had many synapses (Wang et al., 2002; Weiner et al., 2005). Moreover, our neuronal cultures are fed with culture medium conditioned by astrocytes, but are devoid of contacting astrocytes since only 6% of the neurons in these cultures have a contacting astrocyte (Y. Li et al., 2010). The results indicate that neither the presence of contacting astrocytes nor expression of Pcdh-γC (or other Pcdh-γs) are essential for neuronal synaptogenesis.

Nevertheless, the frequent apposition of Pcdh-γC4 and Pcdh-γC5 puncta to synapses suggests a synaptic supportive role. This interpretation is consistent with those in which the selective deletion of the Pcdh-γ family in astrocytes delays, but does not prevent, the formation of both excitatory and inhibitory synapses in spinal cord neurons (Garrett &

Weiner, 2009). It has also recently been reported that homophilic neuron-astrocyte Pcdh interactions promote dendritic arborization complexity in a non-autonomous way (Molumby et al., 2016). The possible involvement of homophilic Pcdh-γC4 (and/or the other two Pcdh-γCs) neuron/astrocyte trans-interactions in dendritic complexity has not been studied to this date.

The apposition of Pcdh-γC4 puncta to GABAergic and glutamatergic synapses and the association of a subpopulation of Pcdh-γC4 puncta with neuron-astrocyte contacts suggest an important role of Pcdh-γC4 in the tri-partite synapse, a functional unit comprising the pre and post-synaptic neuronal elements and a surrounding astrocytic process (Araque, Parpura, Sanzgiri, & Haydon, 1999). This arrangement in the cerebral cortex (Fig. 12k–m and Fig. 13) and hippocampus functionally separates individual synapses by the astrocyte process, efficiently removing released GABA and glutamate from the synapse. In the granule cell layer of the cerebellum, astrocyte processes separate synaptic glomeruli from each other and from the soma of granule cells. Moreover, the contacts between astrocyte processes and synaptic glomeruli or granule cell somas show many Pcdh-γC4 puncta (Fig. 14g). This arrangement functionally separates individual synaptic glomeruli and glomeruli from granule cell somas.

Another structure heavily surrounded by astrocytic processes and enriched in Pcdh-γC4 is the “pinceau” of the basket cell axon synapsing onto the AIS of Purkinje cell (Figs. 12a and 14d and E). This arrangement functionally separates not only the pinceau of a Purkinje cell from the pinceau of a neighboring Purkinje cell, but also from the nearby synaptic glomeruli of the granule cell layer (Fig. 12a and 14d and e). Also, note that the radial Bergmann glia processes of the molecular layer of the cerebellum (Fig. 14 d and f), show Pcdh-γC4 puncta apposed to GABAergic synapses, similar to astrocytes in other brain regions.

Astrocytes and astrocyte processes not only functionally separate individual synapses or synaptic glomeruli, but they also surround and presumably functionally separate individual olfactory glomeruli from each other. Astrocytes and their processes that are present in the periglomerular space show large Pcdh-γC4 puncta in their interface with periglomerular neurons (Fig. 11a, c and e and Fig. 14a). Moreover, astrocyte processes and Pcdh-γC4 puncta are also apposed to synapses inside the glomerulus (Fig. 11a, c and e and Fig. 14a).

An interesting feature of the granule cells of the olfactory bulb (Fig. 11b and d and Fig. 14b) and the granule cells of the cerebellum (Fig. 11h and Fig. 14g) is the formation of cell clusters (Fig. 11b and d) or cell rows (Fig. 11h). The somas of these neurons are in contact with each other without astrocyte processes separating them and with no Pcdh-γC4 puncta between these neurons. It has been shown that these neurons in the olfactory bulb are electrically coupled (Reyher et al., 1991).

It seems that that the presence of astrocyte processes and the presence of Pcdh-γC4 puncta delineate a functional separation not only of individual synapses and synaptic glomeruli, but also of other structures. Pcdh-γC4 concentrates at the boundary between morphologically and functionally different layers in some brain regions. Above we have shown that Pcdh-γC4 concentrates around olfactory glomeruli, separating them (Fig. 10d, Fig. 11a, c and e,

Fig. 14a). Pcdh-γC4 also concentrates between the plexiform and granule layers of the dentate gyrus (Fig. 10e and f, Fig. 12b). Additionally, Pcdh-γC4 concentrates at the boundary between the granule cell layer and molecular layers of the cerebellum (Fig. 10h, i and j, Fig. 11g). Thus, the anti-Pcdh-γC4 Ab can be used as a tool to reveal the organization of functional units defined by neuron-glia interaction at the synaptic level and the identification of clusters of neurons that are synaptically coupled.

Possible roles of Pcdh-γC4 in cell-cell recognition

Different members of the Pcdh-α, Pcdh-β and Pcdh-γ families expressed by a single cell show promiscuous heterophilic cis-interactions with each other, forming cis-heterodimers and/or cis-heterotetramers (Biswas et al., 2012; J. Chen et al., 2009; Han, Lin, Meng, & Wang, 2010; Murata, Hamada, Morishita, Mutoh, & Yagi, 2004; Schalm, Ballif, Buchanan, Phillips, & Maniatis, 2010; Schreiner & Weiner, 2010). In contrast, Pcdh trans-interactions are homophilic. It has been proposed that neuronal diversity results from stochastic expression of Pcdhs and dimeric or tetrameric random combinations of all the cis-interacting Pcdhs expressed by single neurons (Hasegawa et al., 2017; Schreiner & Weiner, 2010; Thu et al., 2014; Yagi, 2012; Zipursky & Sanes, 2010). It has also been proposed that the heterodimers expressed by a single cell would show homophilic antiparallel trans-interaction with identical heterodimers expressed by a contacting cell (Hasegawa et al., 2017; Nicoludis et al., 2015; Nicoludis et al., 2016; Schreiner & Weiner, 2010; Thu et al., 2014; Yagi, 2012; Zipursky & Sanes, 2010). Another model proposes a zipper-like trans-interaction of heterodimers and that this mechanism is involved in self-recognition and self-avoidance of dendrites or axons from the same neuron (Brasch et al., 2019; Goodman et al., 2017; Goodman et al., 2016; Rubinstein, Goodman, Maniatis, Shapiro, & Honig, 2017; Rubinstein et al., 2015).

The probabilistic and combinatorial models (Rubinstein et al., 2017; Schreiner & Weiner, 2010; Thu et al., 2014; Yagi, 2012; Zipursky & Sanes, 2010) of cis-heterodimers that have been proposed to be involved in these trans-homophilic interactions, are based on a random cis-dimeric combinations of all the Pcdhs expressed by a single cell. Some models assume a more restricted number of permissive cis-dimeric combinations involved in homophilic trans-interactions (Thu et al., 2014).

There are other possibilities not considered in the current models: Are changes in the relative level of expression of individual Pcdhs in a neuron, a way to regulate the composition of the cis-heterodimers and trans-interactions? Do cis-heterodimers of different Pcdh composition made by a single neuron segregate into different neuronal compartments such as soma, axon or dendrites? Do the cis-heterodimers expressed by a neuron that are involved in self-avoidance have the same Pcdh composition as the ones involved in trans-homophilic cell-cell adhesion? Moreover, regulation of Pcdh trafficking between the plasma membrane and internal membranes is likely involved in regulating Pcdhs at the cell surface and their trans-interactions (Phillips et al., 2017).

Some of our results provide some insights into these questions. The Pcdh recognition code is likely affected not only by the number of Pcdh-γ mRNA species present in the cytoplasm of a single cell but also by the level of protein expression of individual Pcdhs in that particular

cell relative to other cells. We have found that although all HP neurons show Pcdh-γC4 puncta, the level of expression varies widely even among the same type of neurons (pyramidal cell vs. pyramidal cell or interneuron vs. interneuron). In general, the Pcdh-γC4 expression in interneurons was higher than in pyramidal cells. Therefore, the probabilistic and combinatorial models need to be refined taking into consideration spatial-temporal variations in the levels of protein expression of individual Pcdhs, which would affect the relative number of cis-homo and heterodimers and therefore the repertory of homophilic trans-interactions. The current models do not take into consideration the documented changes in relative expression levels of some Pcdhs during development (Frank et al., 2005; Y. Li et al., 2010). Moreover, the functional role of the Pcdh homophilic trans-interactions between neurons and glia is seldom considered in these models, which mostly addresses neuron-to-neuron recognition or neuron self-recognition.

Our IF results in HP cultures are consistent with the notion, based on mRNA analysis, that the C-type Pcdh-γs are constitutively expressed by most neurons (Esumi et al., 2005; Frank et al., 2005; Hirayama & Yagi, 2017; Kaneko et al., 2006; Wang et al., 2002). We found that in the WT mouse, most neurons showed both Pcdh-γC4 and Pcdh-γA puncta. However, not all but 54–58% of the puncta had both Pcdh-γC4 and Pcdh-γA (Fig. 6). The results are consistent with the notion that i) in neurons that express both Pcdh-γC4 and Pcdh-γA(s), there is heterogeneity in the Pcdh-γ composition of the puncta present in an individual neuron and ii) there is segregation of cis-heterodimers with different Pcdh-γ composition.

Pcdh-γC4 and Pcdh-γC5 are constitutively expressed by most neurons and astrocytes and are concentrated at neuron-astrocyte contact points throughout the brain. It is unlikely that the derived cis-homomers or cis-heteromers involved in promiscuous homophilic trans-interactions would be also specifying neuronal or astrocyte diversity. An astrocyte, which expresses a defined set of Pcdhs, interacts with multiple neurons and could wrap up to several thousand of synapses (Halassa, Fellin, Takano, Dong, & Haydon, 2007; Stogsdill & Eroglu, 2017). Thus, the constitutively expressed Pcdh-γC4 and Pcdh-γC5 in neurons and astrocytes are likely to be involved in general neuronal-astrocyte interactions and not in specifying cell or synaptic identity. In contrast, the non-C-type Pcdh-γs are stochastically expressed (Hirano et al., 2012; Hirayama & Yagi, 2017; Mountoufaris et al., 2017). They might be involved in cell-recognition events where individual neuron identity plays a major role in trans-interactions (i.e. self-avoidance or formation of neuronal circuits).

The distal (C-terminal) part of the cytoplasmic domain of Pcdh-γs is common to all members of the family. In contrast, the part of the cytoplasmic domain that is proximal to the membrane is unique for each Pcdh-γ. Therefore, the extracellular trans-interactions of Pcdh-γ heterodimers made by a cell have the potential for both specific and common signal transduction pathways in the cytoplasmic domain, via protein interactions that are specific for individual Pcdh-γs and/or common to all cis-heterodimers. Intracellular signaling pathways common to many Pcdhs include the focal adhesion kinases PYK2 and FAK, programmed cell death protein 10, PKC, MARCKS, SCG10 and Rho GTPases, among others (J. Chen et al., 2009; Garrett, Schreiner, Lobas, & Weiner, 2012; Gayet, Labella, Henderson, & Kallenbach, 2004; Han et al., 2010; Keeler, Schreiner, & Weiner, 2015; Lin, Meng, Zhu, & Wang, 2010; Suo, Lu, Ying, Capecchi, & Wu, 2012). But there are also Pcdh-

specific cytoplasmic interactions, such as the aforementioned specific interaction between Pcdh-γC5 and $GABA_A$Rs (Y. Li et al., 2012).

Possible Role of Pcdh-γC4 in axon targeting

Olfactory sensory neurons (OSN) require the expression of the three Pcdh families (Pcdh-α, Pcdh-β and Pcdh-γ) for convergence into olfactory glomeruli (Hasegawa et al., 2008; Hasegawa et al., 2012; Hasegawa et al., 2016; Mountoufaris et al., 2017). Individual OSN express unique repertoires of Pcdhs resulting from combinatorial and stochastic expression of members of each of the three families (Mountoufaris et al., 2017). It has been shown that the variability in Pcdh expression prevents axon repulsion, allowing the convergence of axons from different OSN having the same olfactory receptor, into a specific glomerulus (Mountoufaris et al., 2017). In contrast to Purkinje cells and other types of neurons, the OSN do not express Pcdh-γC4, Pcdh-γC5 or any other C-type Pcdh (Goodman et al., 2017; Mountoufaris et al., 2017). We have shown that Pcdh-γC4 (and Pcdh-γC5) are highly expressed in the olfactory bulb, particularly in the olfactory glomeruli (Figs. 10, 11 and 14). The absence of expression of Pcdh-γC4 (and Pcdh-γC5) in OSN and the stochastic expression of other Pcdhs would allow OSN axons to innervate the glomeruli specifically, avoiding the interaction with Pcdh-γC4, which is highly expressed inside and around all of the olfactory glomeruli. This arrangement would allow the specific interaction of the OSN axons with the target glomerulus.

On the other hand, serotonergic neurons project their axon to many regions of the brain. In addition, the same axon makes synapses "*en passant*" to several neurons. The large majority of the serotonergic neurons express Pcdh-αC2 (the only α isoform expressed in these neurons) at high levels, and Pcdh-γC3 and Pcdh-γC4 at lower levels (W. V. Chen et al., 2017). The selective expression of these constitutively expressed C-type Pcdhs by serotonergic neurons could be involved in both axonal tiling and promoting interactions with other neurons and astrocytes throughout the brain (W. V. Chen et al., 2017; Katori et al., 2017).

Acknowledgements:

We thank Ms. Amna Sarwar, Krishna Karunakaran and Megan Burke for their contribution in some experiments. We thank Drs. Weisheng V. Chen, Chan Aye Thu and Tom Maniatis (Columbia University Medical Center, New York) for providing the TCKO mouse and the Pcdh-γC4-mCherry plasmid. We thank Dr. Marcus Frank (University of Freiburg, Freiburg, Germany) for the Pcdh-γC3-EGFP plasmid. We thank Drs. Akiko Nishiyama and Randall S. Walikonis from our department for providing the mAb to S-100β and the chicken anti-PSD-95 respectively. This research was supported by the NIH-NINDS grant R01NS038752 to A.L.D

ABBREVIATIONS:

AA	amino acids
GABA	γ-aminobutyric acid
EGFP	enhanced green fluorescent protein
$GABA_AR$	γ-aminobutyric acid type A receptor

GAD	glutamic acid decarboxylase
GFAP	glial fibrillary acidic protein
GKO	protocadherin-γ KO mouse
GP	guinea pig
HP	hippocampal or hippocampus
IUEP	*in utero* electroporation
KO	knockout
mAb	monoclonal antibody
Ms	mouse
NGS	normal goat serum
Pcdh	protocadherin
Pcdh-γC4	protocadherin γC4
Rb	rabbit
Sh	sheep
TCKO	triple protocadherin-γ C-type KO mouse
VGAT	vesicular GABA transporter
VGLUT1	vesicular glutamate transporter 1

LITERATURE CITED

Araque A, Parpura V, Sanzgiri RP, & Haydon PG (1999). Tripartite synapses: glia, the unacknowledged partner. Trends Neurosci, 22(5), 208–215. doi:10.1016/S0166-2236(98)01349-6 [PubMed: 10322493]

Bai J, Ramos RL, Ackman JB, Thomas AM, Lee RV, & LoTurco JJ (2003). RNAi reveals doublecortin is required for radial migration in rat neocortex. Nat Neurosci, 6(12), 1277–1283. doi:10.1038/nn1153 [PubMed: 14625554]

Biswas S, Emond MR, & Jontes JD (2012). The clustered protocadherins Pcdhalpha and Pcdhgamma form a heteromeric complex in zebrafish. Neuroscience, 219, 280–289. doi:10.1016/j.neuroscience.2012.05.058 [PubMed: 22659564]

Blank M, Triana-Baltzer GB, Richards CS, & Berg DK (2004). Alpha-protocadherins are presynaptic and axonal in nicotinic pathways. Mol Cell Neurosci, 26(4), 530–543. doi:10.1016/j.mcn.2004.04.008 [PubMed: 15276155]

Brasch J, Goodman KM, Noble AJ, Rapp M, Mannepalli S, Bahna F, … Shapiro L (2019). Visualization of clustered protocadherin neuronal self-recognition complexes. Nature. doi:10.1038/s41586-019-1089-3

Charych EI, Yu W, Li R, Serwanski DR, Miralles CP, Li X, … De Blas AL (2004). A four PDZ domain-containing splice variant form of GRIP1 is localized in GABAergic and glutamatergic synapses in the brain. J Biol Chem, 279(37), 38978–38990. doi:10.1074/jbc.M405786200 [PubMed: 15226318]

Charych EI, Yu W, Miralles CP, Serwanski DR, Li X, Rubio M, & De Blas AL (2004). The brefeldin A-inhibited GDP/GTP exchange factor 2, a protein involved in vesicular trafficking, interacts with the beta subunits of the GABA receptors. J Neurochem, 90(1), 173–189. doi:10.1111/j.1471-4159.2004.02481.x [PubMed: 15198677]

Chen F, & LoTurco J (2012). A method for stable transgenesis of radial glia lineage in rat neocortex by piggyBac mediated transposition. J Neurosci Methods, 207(2), 172–180. doi:10.1016/j.jneumeth.2012.03.016 [PubMed: 22521325]

Chen J, Lu Y, Meng S, Han MH, Lin C, & Wang X (2009). alpha- and gamma-Protocadherins negatively regulate PYK2. J Biol Chem, 284(5), 2880–2890. doi:10.1074/jbc.M807417200 [PubMed: 19047047]

Chen WV, Alvarez FJ, Lefebvre JL, Friedman B, Nwakeze C, Geiman E, … Maniatis T (2012). Functional significance of isoform diversification in the protocadherin gamma gene cluster. Neuron, 75(3), 402–409. doi:10.1016/j.neuron.2012.06.039 [PubMed: 22884324]

Chen WV, & Maniatis T (2013). Clustered protocadherins. Development, 140(16), 3297–3302. doi:10.1242/dev.090621 [PubMed: 23900538]

Chen WV, Nwakeze CL, Denny CA, O'Keeffe S, Rieger MA, Mountoufaris G, … Maniatis T (2017). Pcdhalphac2 is required for axonal tiling and assembly of serotonergic circuitries in mice. Science, 356(6336), 406–411. doi:10.1126/science.aal3231 [PubMed: 28450636]

Chiou TT, Bonhomme B, Jin H, Miralles CP, Xiao H, Fu Z, … De Blas AL (2011). Differential regulation of the postsynaptic clustering of gamma-aminobutyric acid type A (GABAA) receptors by collybistin isoforms. J Biol Chem, 286(25), 22456–22468. doi:10.1074/jbc.M111.236190 [PubMed: 21540179]

Christie SB, & de Blas AL (2002). alpha5 Subunit-containing GABA(A) receptors form clusters at GABAergic synapses in hippocampal cultures. Neuroreport, 13(17), 2355–2358. doi:10.1097/01.wnr.0000045008.30898.dd [PubMed: 12488826]

Christie SB, & De Blas AL (2003). GABAergic and glutamatergic axons innervate the axon initial segment and organize GABA(A) receptor clusters of cultured hippocampal pyramidal cells. J Comp Neurol, 456(4), 361–374. doi:10.1002/cne.10535 [PubMed: 12532408]

Christie SB, Li RW, Miralles CP, Riquelme R, Yang BY, Charych E, … De Blas AL (2002). Synaptic and extrasynaptic GABAA receptor and gephyrin clusters. Prog Brain Res, 136, 157–180. doi:10.1016/S0079-6123(02)36015-1 [PubMed: 12143379]

Christie SB, Li RW, Miralles CP, Yang B, & De Blas AL (2006). Clustered and non-clustered GABAA receptors in cultured hippocampal neurons. Mol Cell Neurosci, 31(1), 1–14. doi:10.1016/j.mcn.2005.08.014 [PubMed: 16181787]

Christie SB, Miralles CP, & De Blas AL (2002). GABAergic innervation organizes synaptic and extrasynaptic GABAA receptor clustering in cultured hippocampal neurons. J Neurosci, 22(3), 684–697. doi:10.1523/JNEUROSCI.22-03-00684.2002 [PubMed: 11826098]

de Blas AL (1984). Monoclonal antibodies to specific astroglial and neuronal antigens reveal the cytoarchitecture of the Bergmann glia fibers in the cerebellum. J Neurosci, 4(1), 265–273. doi:10.1523/JNEUROSCI.04-01-00265.1984 [PubMed: 6693942]

De Blas AL, & Cherwinski HM (1983). Detection of antigens on nitrocellulose paper immunoblots with monoclonal antibodies. Anal Biochem, 133(1), 214–219. doi:10.1016/0003-2697(83)90245-2 [PubMed: 6356979]

Esumi S, Kakazu N, Taguchi Y, Hirayama T, Sasaki A, Hirabayashi T, … Yagi T (2005). Monoallelic yet combinatorial expression of variable exons of the protocadherin-alpha gene cluster in single neurons. Nat Genet, 37(2), 171–176. doi:10.1038/ng1500 [PubMed: 15640798]

Fekete CD, Chiou TT, Miralles CP, Harris RS, Fiondella CG, Loturco JJ, & De Blas AL (2015). In vivo clonal overexpression of neuroligin 3 and neuroligin 2 in neurons of the rat cerebral cortex: Differential effects on GABAergic synapses and neuronal migration. J Comp Neurol, 523(9), 1359–1378. doi:10.1002/cne.23740 [PubMed: 25565602]

Fekete CD, Goz RU, Dinallo S, Miralles CP, Chiou TT, Bear J Jr., … De Blas AL (2017). In vivo transgenic expression of collybistin in neurons of the rat cerebral cortex. J Comp Neurol, 525(5), 1291–1311. doi:10.1002/cne.24137 [PubMed: 27804142]

Fernandez-Monreal M, Kang S, & Phillips GR (2009). Gamma-protocadherin hemophilic interaction and intracellular trafficking is controlled by the cytoplasmic domain in neurons. Mol Cell Neurosci, 40(3), 344–353. doi:10.1016/j.mcn.2008.12.002 [PubMed: 19136062]

Fernandez-Monreal M, Oung T, Hanson HH, O'Leary R, Janssen WG, Dolios G, … Phillips GR (2010). gamma-protocadherins are enriched and transported in specialized vesicles associated with the secretory pathway in neurons. Eur J Neurosci, 32(6), 921–931. doi:10.1111/j.1460-9568.2010.07386.x [PubMed: 20849527]

Frank M, Ebert M, Shan W, Phillips GR, Arndt K, Colman DR, & Kemler R (2005). Differential expression of individual gamma-protocadherins during mouse brain development. Mol Cell Neurosci, 29(4), 603–616. doi:10.1016/j.mcn.2005.05.001 [PubMed: 15964765]

Garrett AM, Schreiner D, Lobas MA, & Weiner JA (2012). gamma-protocadherins control cortical dendrite arborization by regulating the activity of a FAK/PKC/MARCKS signaling pathway. Neuron, 74(2), 269–276. doi:10.1016/j.neuron.2012.01.028 [PubMed: 22542181]

Garrett AM, & Weiner JA (2009). Control of CNS synapse development by {gamma}-protocadherin-mediated astrocyte-neuron contact. J Neurosci, 29(38), 11723–11731. doi:10.1523/JNEUROSCI.2818-09.2009 [PubMed: 19776259]

Gayet O, Labella V, Henderson CE, & Kallenbach S (2004). The b1 isoform of protocadherin-gamma (Pcdhgamma) interacts with the microtubule-destabilizing protein SCG10. FEBS Lett, 578(1–2), 175–179. doi:10.1016/j.febslet.2004.10.096 [PubMed: 15581637]

Goodman KM, Rubinstein R, Dan H, Bahna F, Mannepalli S, Ahlsen G, … Shapiro L (2017). Protocadherin cis-dimer architecture and recognition unit diversity. Proc Natl Acad Sci U S A, 114(46), E9829–E9837. doi:10.1073/pnas.1713449114 [PubMed: 29087338]

Goodman KM, Rubinstein R, Thu CA, Bahna F, Mannepalli S, Ahlsen G, … Shapiro L (2016). Structural Basis of Diverse Homophilic Recognition by Clustered alpha- and beta-Protocadherins. Neuron, 90(4), 709–723. doi:10.1016/j.neuron.2016.04.004 [PubMed: 27161523]

Halassa MM, Fellin T, Takano H, Dong JH, & Haydon PG (2007). Synaptic islands defined by the territory of a single astrocyte. J Neurosci, 27(24), 6473–6477. doi:10.1523/JNEUROSCI.1419-07.2007 [PubMed: 17567808]

Han MH, Lin C, Meng S, & Wang X (2010). Proteomics analysis reveals overlapping functions of clustered protocadherins. Mol Cell Proteomics, 9(1), 71–83. doi:10.1074/mcp.M900343-MCP200 [PubMed: 19843561]

Hasegawa S, Hamada S, Kumode Y, Esumi S, Katori S, Fukuda E, … Yagi T (2008). The protocadherin-alpha family is involved in axonal coalescence of olfactory sensory neurons into glomeruli of the olfactory bulb in mouse. Mol Cell Neurosci, 38(1), 66–79. doi:10.1016/j.mcn.2008.01.016 [PubMed: 18353676]

Hasegawa S, Hirabayashi T, Kondo T, Inoue K, Esumi S, Okayama A, … Yagi T (2012). Constitutively expressed Protocadherin-alpha regulates the coalescence and elimination of homotypic olfactory axons through its cytoplasmic region. Front Mol Neurosci, 5, 97. doi:10.3389/fnmol.2012.00097 [PubMed: 23087612]

Hasegawa S, Kobayashi H, Kumagai M, Nishimaru H, Tarusawa E, Kanda H, … Yagi T (2017). Clustered Protocadherins Are Required for Building Functional Neural Circuits. Front Mol Neurosci, 10, 114. doi:10.3389/fnmol.2017.00114 [PubMed: 28484370]

Hasegawa S, Kumagai M, Hagihara M, Nishimaru H, Hirano K, Kaneko R, … Yagi T (2016). Distinct and Cooperative Functions for the Protocadherin-alpha, -beta and -gamma Clusters in Neuronal Survival and Axon Targeting. Front Mol Neurosci, 9, 155. doi:10.3389/fnmol.2016.00155 [PubMed: 28066179]

Hayashi S, & Takeichi M (2015). Emerging roles of protocadherins: from self-avoidance to enhancement of motility. J Cell Sci, 128(8), 1455–1464. doi:10.1242/jcs.166306 [PubMed: 25749861]

Higgins D, and Banker G (1998) in Culturing Nerve Cells (Banker G and Goslin K, eds) 2nd Ed., pp. 37–78, MIT Press, Cambridge, MA

Hirano K, Kaneko R, Izawa T, Kawaguchi M, Kitsukawa T, & Yagi T (2012). Single-neuron diversity generated by Protocadherin-beta cluster in mouse central and peripheral nervous systems. Front Mol Neurosci, 5, 90. doi:10.3389/fnmol.2012.00090 [PubMed: 22969705]

Hirayama T, & Yagi T (2013). Clustered protocadherins and neuronal diversity. Prog Mol Biol Transl Sci, 116, 145–167. doi:10.1016/B978-0-12-394311-8.00007-8 [PubMed: 23481194]

Hirayama T, & Yagi T (2017). Regulation of clustered protocadherin genes in individual neurons. Semin Cell Dev Biol. doi:10.1016/j.semcdb.2017.05.026

Jin H, Chiou TT, Serwanski DR, Miralles CP, Pinal N, & De Blas AL (2014). Ring finger protein 34 (RNF34) interacts with and promotes gamma-aminobutyric acid type-A receptor degradation via ubiquitination of the gamma2 subunit. J Biol Chem, 289(42), 29420–29436. doi:10.1074/jbc.M114.603068 [PubMed: 25193658]

Kaneko R, Kato H, Kawamura Y, Esumi S, Hirayama T, Hirabayashi T, & Yagi T (2006). Allelic gene regulation of Pcdh-alpha and Pcdh-gamma clusters involving both monoallelic and biallelic expression in single Purkinje cells. J Biol Chem, 281(41), 30551–30560. doi:10.1074/jbc.M605677200 [PubMed: 16893882]

Katori S, Noguchi-Katori Y, Okayama A, Kawamura Y, Luo W, Sakimura K, … Yagi T (2017). Protocadherin-alphaC2 is required for diffuse projections of serotonergic axons. Sci Rep, 7(1), 15908. doi:10.1038/s41598-017-16120-y [PubMed: 29162883]

Keeler AB, Molumby MJ, & Weiner JA (2015). Protocadherins branch out: Multiple roles in dendrite development. Cell Adh Migr, 9(3), 214–226. doi:10.1080/19336918.2014.1000069 [PubMed: 25869446]

Keeler AB, Schreiner D, & Weiner JA (2015). Protein Kinase C Phosphorylation of a gamma-Protocadherin C-terminal Lipid Binding Domain Regulates Focal Adhesion Kinase Inhibition and Dendrite Arborization. J Biol Chem, 290(34), 20674–20686. doi:10.1074/jbc.M115.642306 [PubMed: 26139604]

Lefebvre JL (2017). Neuronal territory formation by the atypical cadherins and clustered protocadherins. Semin Cell Dev Biol, 69, 111–121. doi:10.1016/j.semcdb.2017.07.040 [PubMed: 28756270]

Lefebvre JL, Zhang Y, Meister M, Wang X, & Sanes JR (2008). gamma-Protocadherins regulate neuronal survival but are dispensable for circuit formation in retina. Development, 135(24), 4141–4151. doi:10.1242/dev.027912 [PubMed: 19029044]

Li X, Serwanski DR, Miralles CP, Nagata K, & De Blas AL (2009). Septin 11 is present in GABAergic synapses and plays a functional role in the cytoarchitecture of neurons and GABAergic synaptic connectivity. J Biol Chem, 284(25), 17253–17265. [PubMed: 19380581]

Li Y, Chen Z, Gao Y, Pan G, Zheng H, Zhang Y, … Zheng H (2017). Synaptic Adhesion Molecule Pcdh-gammaC5 Mediates Synaptic Dysfunction in Alzheimer's Disease. J Neurosci, 37(38), 9259–9268. doi:10.1523/JNEUROSCI.1051-17.2017 [PubMed: 28842416]

Li Y, Serwanski DR, Miralles CP, Fiondella CG, Loturco JJ, Rubio ME, & De Blas AL (2010). Synaptic and nonsynaptic localization of protocadherin-gammaC5 in the rat brain. J Comp Neurol, 518(17), 3439–3463. doi:10.1002/cne.22390 [PubMed: 20589908]

Li Y, Xiao H, Chiou TT, Jin H, Bonhomme B, Miralles CP, … De Blas AL (2012). Molecular and functional interaction between protocadherin-gammaC5 and GABAA receptors. J Neurosci, 32(34), 11780–11797. doi:10.1523/JNEUROSCI.0969-12.2012 [PubMed: 22915120]

Light SEW, & Jontes JD (2017). delta-Protocadherins: Organizers of neural circuit assembly. Semin Cell Dev Biol, 69, 83–90. doi:10.1016/j.semcdb.2017.07.037 [PubMed: 28751249]

Lin C, Meng S, Zhu T, & Wang X (2010). PDCD10/CCM3 acts downstream of {gamma}-protocadherins to regulate neuronal survival. J Biol Chem, 285(53), 41675–41685. doi:10.1074/jbc.M110.179895 [PubMed: 21041308]

Mah KM, Houston DW, & Weiner JA (2016). The gamma-Protocadherin-C3 isoform inhibits canonical Wnt signalling by binding to and stabilizing Axin1 at the membrane. Sci Rep, 6, 31665. doi:10.1038/srep31665 [PubMed: 27530555]

Molumby MJ, Anderson RM, Newbold DJ, Koblesky NK, Garrett AM, Schreiner D, … Weiner JA (2017). gamma-Protocadherins Interact with Neuroligin-1 and Negatively Regulate Dendritic Spine Morphogenesis. Cell Rep, 18(11), 2702–2714. doi:10.1016/j.celrep.2017.02.060 [PubMed: 28297673]

Molumby MJ, Keeler AB, & Weiner JA (2016). Homophilic Protocadherin Cell-Cell Interactions Promote Dendrite Complexity. Cell Rep, 15(5), 1037–1050. doi:10.1016/j.celrep.2016.03.093 [PubMed: 27117416]

Mountoufaris G, Canzio D, Nwakeze CL, Chen WV, & Maniatis T (2018). Writing, Reading, and Translating the Clustered Protocadherin Cell Surface Recognition Code for Neural Circuit Assembly. Annu Rev Cell Dev Biol, 34, 471–493. doi:10.1146/annurev-cellbio-100616-060701 [PubMed: 30296392]

Mountoufaris G, Chen WV, Hirabayashi Y, O'Keeffe S, Chevee M, Nwakeze CL, … Maniatis T (2017). Multicluster Pcdh diversity is required for mouse olfactory neural circuit assembly. Science, 356(6336), 411–414. doi:10.1126/science.aai8801 [PubMed: 28450637]

Murata Y, Hamada S, Morishita H, Mutoh T, & Yagi T (2004). Interaction with protocadherin-gamma regulates the cell surface expression of protocadherin-alpha. J Biol Chem, 279(47), 49508–49516. doi:10.1074/jbc.M408771200 [PubMed: 15347688]

Nicoludis JM, Lau SY, Scharfe CP, Marks DS, Weihofen WA, & Gaudet R (2015). Structure and Sequence Analyses of Clustered Protocadherins Reveal Antiparallel Interactions that Mediate Homophilic Specificity. Structure, 23(11), 2087–2098. doi:10.1016/j.str.2015.09.005 [PubMed: 26481813]

Nicoludis JM, Vogt BE, Green AG, Scharfe CP, Marks DS, & Gaudet R (2016). Antiparallel protocadherin homodimers use distinct affinity- and specificity-mediating regions in cadherin repeats 1–4. Elife, 5. doi:10.7554/eLife.18449

Oertel WH, Schmechel DE, Mugnaini E, Tappaz ML, & Kopin IJ (1981). Immunocytochemical localization of glutamate decarboxylase in rat cerebellum with a new antiserum. Neuroscience, 6(12), 2715–2735. doi:10.1016/0306-4522(81)90115-9 [PubMed: 7033824]

Oertel WH, Schmechel DE, Tappaz ML, & Kopin IJ (1981). Production of a specific antiserum to rat brain glutamic acid decarboxylase by injection of an antigen-antibody complex. Neuroscience, 6(12), 2689–2700. doi:10.1016/0306-4522(81)90113-5 [PubMed: 7322358]

Peek SL, Mah KM, & Weiner JA (2017). Regulation of neural circuit formation by protocadherins. Cell Mol Life Sci. doi:10.1007/s00018-017-2572-3

Phillips GR, LaMassa N, & Nie YM (2017). Clustered protocadherin trafficking. Semin Cell Dev Biol, 69, 131–139. doi:10.1016/j.semcdb.2017.05.001 [PubMed: 28478299]

Phillips GR, Tanaka H, Frank M, Elste A, Fidler L, Benson DL, & Colman DR (2003). Gamma-protocadherins are targeted to subsets of synapses and intracellular organelles in neurons. J Neurosci, 23(12), 5096–5104. doi:10.1523/JNEUROSCI.23-12-05096.2003 [PubMed: 12832533]

Prasad T, Wang X, Gray PA, & Weiner JA (2008). A differential developmental pattern of spinal interneuron apoptosis during synaptogenesis: insights from genetic analyses of the protocadherin-gamma gene cluster. Development, 135(24), 4153–4164. doi:10.1242/dev.026807 [PubMed: 19029045]

Ramos RL, Bai J, & LoTurco JJ (2006). Heterotopia formation in rat but not mouse neocortex after RNA interference knockdown of DCX. Cereb Cortex, 16(9), 1323–1331. doi:10.1093/cercor/bhj074 [PubMed: 16292002]

Reyher CK, Lubke J, Larsen WJ, Hendrix GM, Shipley MT, & Baumgarten HG (1991). Olfactory bulb granule cell aggregates: morphological evidence for interperikaryal electrotonic coupling via gap junctions. J Neurosci, 11(6), 1485–1495. doi:10.1523/JNEUROSCI.11-06-01485.1991 [PubMed: 1904478]

Rubinstein R, Goodman KM, Maniatis T, Shapiro L, & Honig B (2017). Structural origins of clustered protocadherin-mediated neuronal barcoding. Semin Cell Dev Biol. doi:10.1016/j.semcdb.2017.07.023

Rubinstein R, Thu CA, Goodman KM, Wolcott HN, Bahna F, Mannepalli S, … Honig B (2015). Molecular Logic of Neuronal Self-Recognition through Protocadherin Domain Interactions. Cell, 163(3), 629–642. doi:10.1016/j.cell.2015.09.026 [PubMed: 26478182]

Schalm SS, Ballif BA, Buchanan SM, Phillips GR, & Maniatis T (2010). Phosphorylation of protocadherin proteins by the receptor tyrosine kinase Ret. Proc Natl Acad Sci U S A, 107(31), 13894–13899. doi:10.1073/pnas.1007182107 [PubMed: 20616001]

Schreiner D, & Weiner JA (2010). Combinatorial homophilic interaction between gamma-protocadherin multimers greatly expands the molecular diversity of cell adhesion. Proc Natl Acad Sci U S A, 107(33), 14893–14898. doi:10.1073/pnas.1004526107 [PubMed: 20679223]

Shonubi A, Roman C, & Phillips GR (2015). The clustered protocadherin endolysosomal trafficking motif mediates cytoplasmic association. BMC Cell Biol, 16(1), 28. doi:10.1186/s12860-015-0074-4 [PubMed: 26608278]

Stogsdill JA, & Eroglu C (2017). The interplay between neurons and glia in synapse development and plasticity. Curr Opin Neurobiol, 42, 1–8. doi:10.1016/j.conb.2016.09.016 [PubMed: 27788368]

Suo L, Lu H, Ying G, Capecchi MR, & Wu Q (2012). Protocadherin clusters and cell adhesion kinase regulate dendrite complexity through Rho GTPase. J Mol Cell Biol, 4(6), 362–376. doi:10.1093/jmcb/mjs034 [PubMed: 22730554]

Tasic B, Nabholz CE, Baldwin KK, Kim Y, Rueckert EH, Ribich SA, … Maniatis T (2002). Promoter choice determines splice site selection in protocadherin alpha and gamma pre-mRNA splicing. Mol Cell, 10(1), 21–33. doi:10.1016/S1097-2765(02)00578-6 [PubMed: 12150904]

Thu CA, Chen WV, Rubinstein R, Chevee M, Wolcott HN, Felsovalyi KO, … Maniatis T (2014). Single-cell identity generated by combinatorial homophilic interactions between alpha, beta, and gamma protocadherins. Cell, 158(5), 1045–1059. doi:10.1016/j.cell.2014.07.012 [PubMed: 25171406]

Wang X, Weiner JA, Levi S, Craig AM, Bradley A, & Sanes JR (2002). Gamma protocadherins are required for survival of spinal interneurons. Neuron, 36(5), 843–854. doi:10.1016/S0896-6273(02)01090-5 [PubMed: 12467588]

Weiner JA, & Jontes JD (2013). Protocadherins, not prototypical: a complex tale of their interactions, expression, and functions. Front Mol Neurosci, 6, 4. doi:10.3389/fnmol.2013.00004 [PubMed: 23515683]

Weiner JA, Wang X, Tapia JC, & Sanes JR (2005). Gamma protocadherins are required for synaptic development in the spinal cord. Proc Natl Acad Sci U S A, 102(1), 8–14. doi:10.1073/pnas.0407931101 [PubMed: 15574493]

Wu Q (2005). Comparative genomics and diversifying selection of the clustered vertebrate protocadherin genes. Genetics, 169(4), 2179–2188. doi:10.1534/genetics.104.037606 [PubMed: 15744052]

Wu Q, & Maniatis T (1999). A striking organization of a large family of human neural cadherin-like cell adhesion genes. Cell, 97(6), 779–790. doi:10.1016/S0092-8674(00)80789-8 [PubMed: 10380929]

Wu Q, Zhang T, Cheng JF, Kim Y, Grimwood J, Schmutz J, … Maniatis T (2001). Comparative DNA sequence analysis of mouse and human protocadherin gene clusters. Genome Res, 11(3), 389–404. doi:10.1101/gr.167301 [PubMed: 11230163]

Yagi T (2012). Molecular codes for neuronal individuality and cell assembly in the brain. Front Mol Neurosci, 5, 45. doi:10.3389/fnmol.2012.00045 [PubMed: 22518100]

Yamagata K, Andreasson KI, Sugiura H, Maru E, Dominique M, Irie Y, … Worley PF (1999). Arcadlin is a neural activity-regulated cadherin involved in long term potentiation. J Biol Chem, 274(27), 19473–11979. doi:10.1074/jbc.274.27.19473 [PubMed: 10383464]

Yasuda S, Tanaka H, Sugiura H, Okamura K, Sakaguchi T, Tran U, … Yamagata K (2007). Activity-induced protocadherin arcadlin regulates dendritic spine number by triggering N-cadherin endocytosis via TAO2beta and p38 MAP kinases. Neuron, 56(3), 456–471. doi:10.1016/j.neuron.2007.08.020 [PubMed: 17988630]

Zipursky SL, & Sanes JR (2010). Chemoaffinity revisited: dscams, protocadherins, and neural circuit assembly. Cell, 143(3), 343–353. doi:10.1016/j.cell.2010.10.009 [PubMed: 21029858]

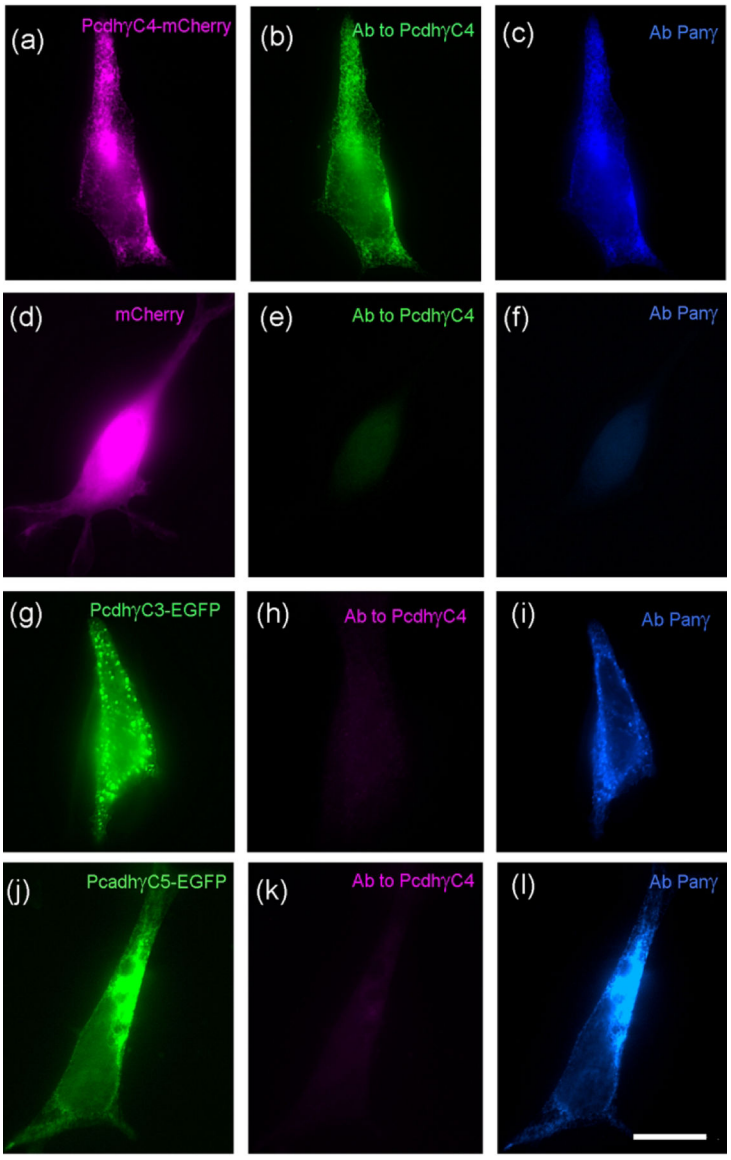

Fig. 1. The anti-Pcdh-γC4 antibody recognizes Pcdh-γC4 but not the other Pcdh-γCs.

(a-l) triple-label immunofluorescence of HEK293 cells transfected with Pcdh-γC4-mCherry (a-c); mCherry (d-f); Pcdh-γC3-EGFP (g-i) or Pcdh-γC5-EGFP (j-l). Panels a and d show mCherry fluorescence (magenta). Panels g and j show EGFP fluorescence (green). The Rb anti-Pcdh-γC4 antibody (green in b and e or magenta in h and k) recognizes Pcdh-γC4-mCherry (b) but not mCherry (e), Pcdh-γC3-EGFP (h) or Pcdh-γC5-EGFP (k). A Ms anti-Pan γ mAb recognizes the thee C-type Pcdh-γs (blue c, i and l) but not mCherry (f). Scale bar = 20 μm.

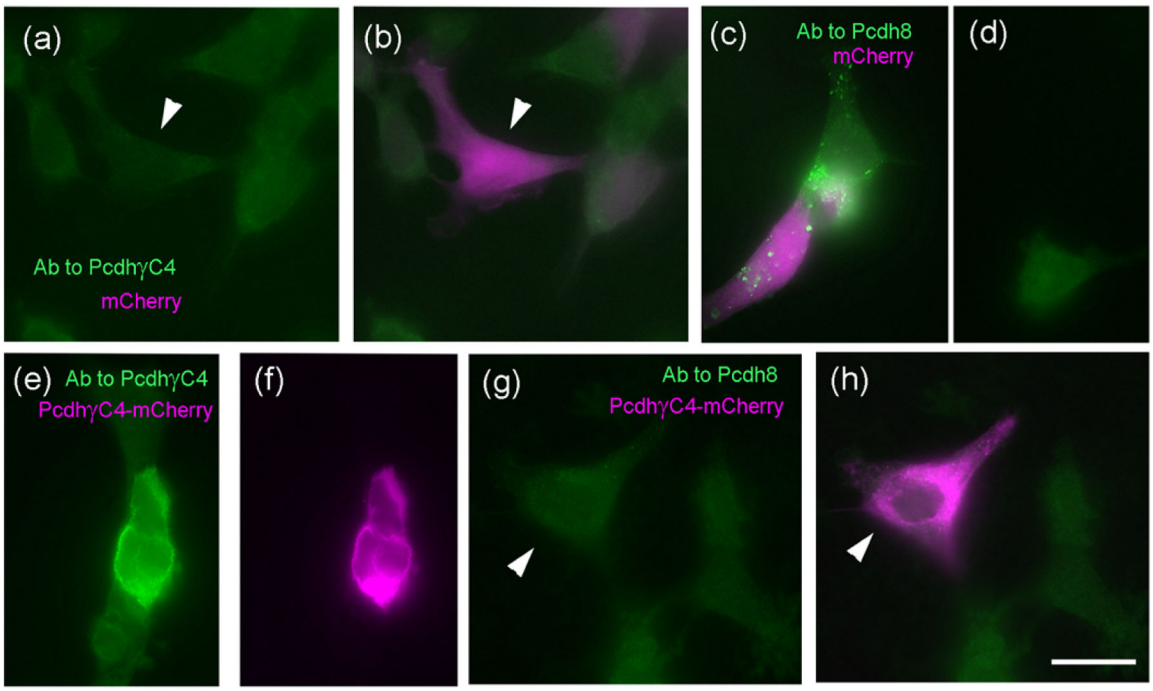

Fig. 2. The anti-Pcdh-γC4 antibody does not recognize Pcdh8.

(a-d) HEK293 cells cotransfected with Pcdh8 and mCherry (magenta). Panels a and b (same cells) show that anti-Pcdh-γC4 Ab (green) does not recognize cells co-transfected with Pcdh8 and mCherry (arrowhead). In contrast, co-transfected cells are recognized by the anti-Pcdh8 antibody (c, green). Panel d shows the absence of green Pcdh8 immunofluorescence in a non-transfected cell (not expressing mCherry). **(e-h)** HEK293 cells transfected with Pcdh-γC4-mCherry. Panels e and f show that the anti-Pcdh-γC4 antibody (e, green) reacts with the transfected cell (f, mCherry magenta). However, the anti-Pcdh8 Ab (green) does not react (g and h) with the transfected cell (arrowhead). Scale bar = 20 μm.

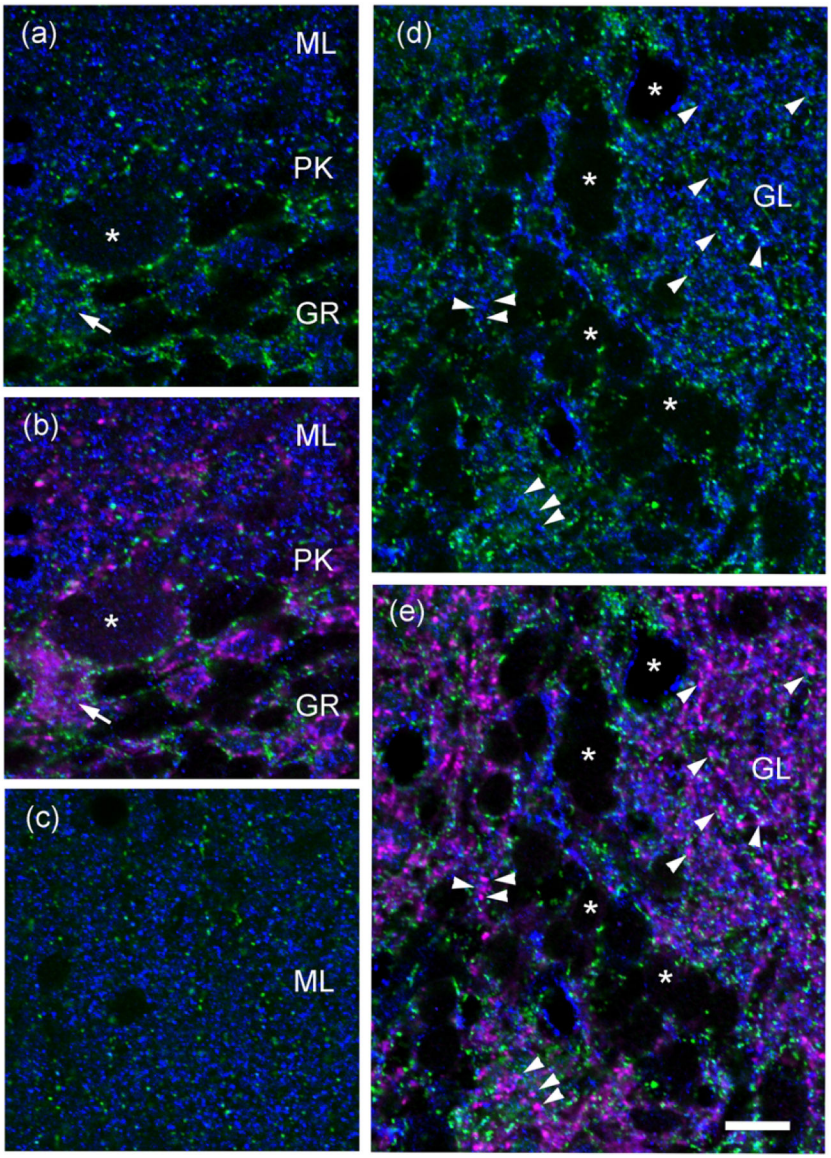

Fig. 3. Double-label Immunofluorescence in brain sections show that anti-Pcdh-γC4 and anti-Pcdh8 labeling do not co-localize.

Triple-label immunofluorescence with Rb anti-Pcdh-γC4 (green), Ms anti-Pcah8 (blue) and GP anti-VGAT (magenta). **(a and b)** are the same field of Purkinje cell layer (PK), molecular layer (ML) and granule cell layer (GR) of the cerebellum. The asterisk marks a Purkinje cell and the arrow the corresponding GABAergic pinceaux in the AIS (magenta). **(c)** ML layer of the cerebellum. While Pcdh-γC4 immunofluorescence concentrates in the Bergmann glia processes (green, vertical alignments), Pcdh8 immunofluorescence (blue) profusely labels the neuropil of the ML. **(d-e)** olfactory bulb. GL indicates an olfactory glomerulus. Asterisks indicate some periglomerular neurons. Arrowheads point to co-localization of VGAT-terminals (magenta) with Pcdh8 (blue). Pcdh-γC4 puncta (green) are adjacent to VGAT-terminals. There is little co-localization between Pcdh-γC4 and Pcdh8. Scale bar = 10 μm.

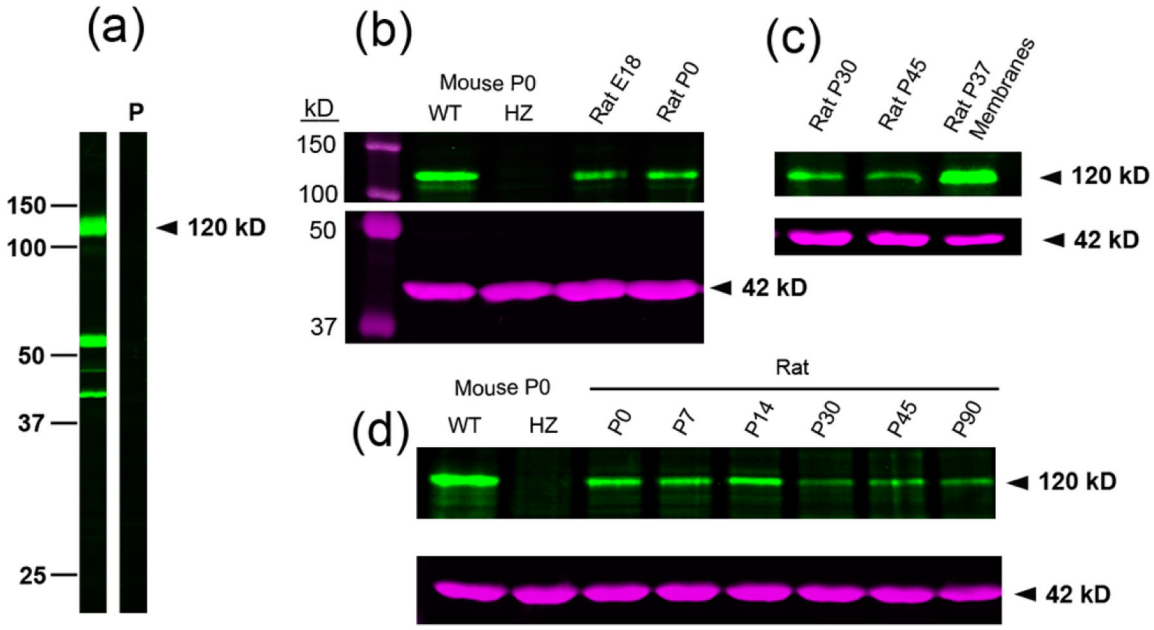

Fig. 4. Immunoblots of rat and mouse brain tissue with anti-Pcdh-γC4.

(a) Rat forebrain membranes from P37 show three main protein bands of 120, 55 and 40 kD. The immunoreaction with the three proteins is blocked with 20 μg/ml of peptide antigen (strip P). They are two nitrocellulose strips from the same transfer processed in parallel, under the same conditions. The mobility of Mw markers (in kD) is shown at the left. **(b)** Comparative expression of the 120 kD Pcdh-γC4 protein as revealed with anti-Pcdh-γC4 (green). The left lane shows the mobility of Mw protein markers (150 and 100 kD, magenta). Next two left lanes show P0 cleared brain homogenates of wild type (WT) and homozygous (HZ) mutant TCKO mouse. Right side lanes show cleared homogenates of E18 and P0 rat brains. Underneath (magenta) shows the immunoblot of the same lanes with anti-β-actin antibody, revealing a 42 kD β-actin protein band that migrates between the 50 and 37 kD protein markers, (left lane). **(c)** The 120 kD Pcdh-γC4 protein (green) is expressed in the P30 and P45 rat brain cleared homogenates. Also, note the enrichment of the 120 kD Pcdh-γC4 protein in the membranes of the P37 rat brain. **(d)** Developmental expression of the 120 kD Pcdh-γC4 protein in the rat brain. The left lanes show the WT and HZ TCKO mice, for protein band identification. Underneath, in magenta, are the same lanes with anti-β-actin. Same amount of total protein was added in each lane (40 μg).

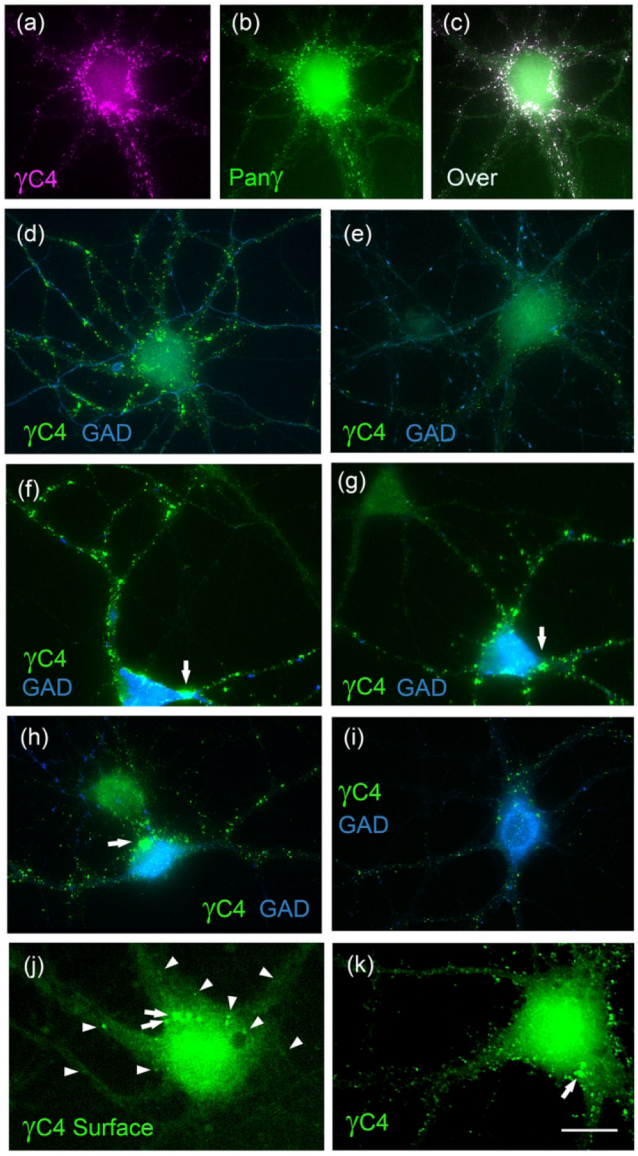

Fig. 5. Pcdh-γC4 is expressed in cultured rat HP neurons forming puncta.

(a-c) Double-label immunofluorescence with the Rb anti-Pcdh-γC4 (γC4, magenta) and Ms anti-pan-Pcdh-γ (Panγ, green). Panel c shows the overlay (Over). **(d-i)** Double-label immunofluorescence with the Rb anti-Pcdh-γC4 (green) and sheep anti-GAD (blue). Panels d and e show GAD-glutamatergic pyramidal neurons. Panels f-i show GAD+ GABAergic interneurons. Arrows point to very large Pcdh-γC4 puncta present in some interneurons. **(j-k)** Immunofluorescence with Rb anti-Pcdh-γC4 (γC4, green) of non-permeabilized surface-labelled (j) and permeabilized (k) neurons from the same experiment. Arrowheads point to Pcdh-γC4 puncta in surface-labeled neurons. Arrows point to large Pcdh-γC4 puncta. Scale bar = 20 μm for a-i and 10 μm for j-k.

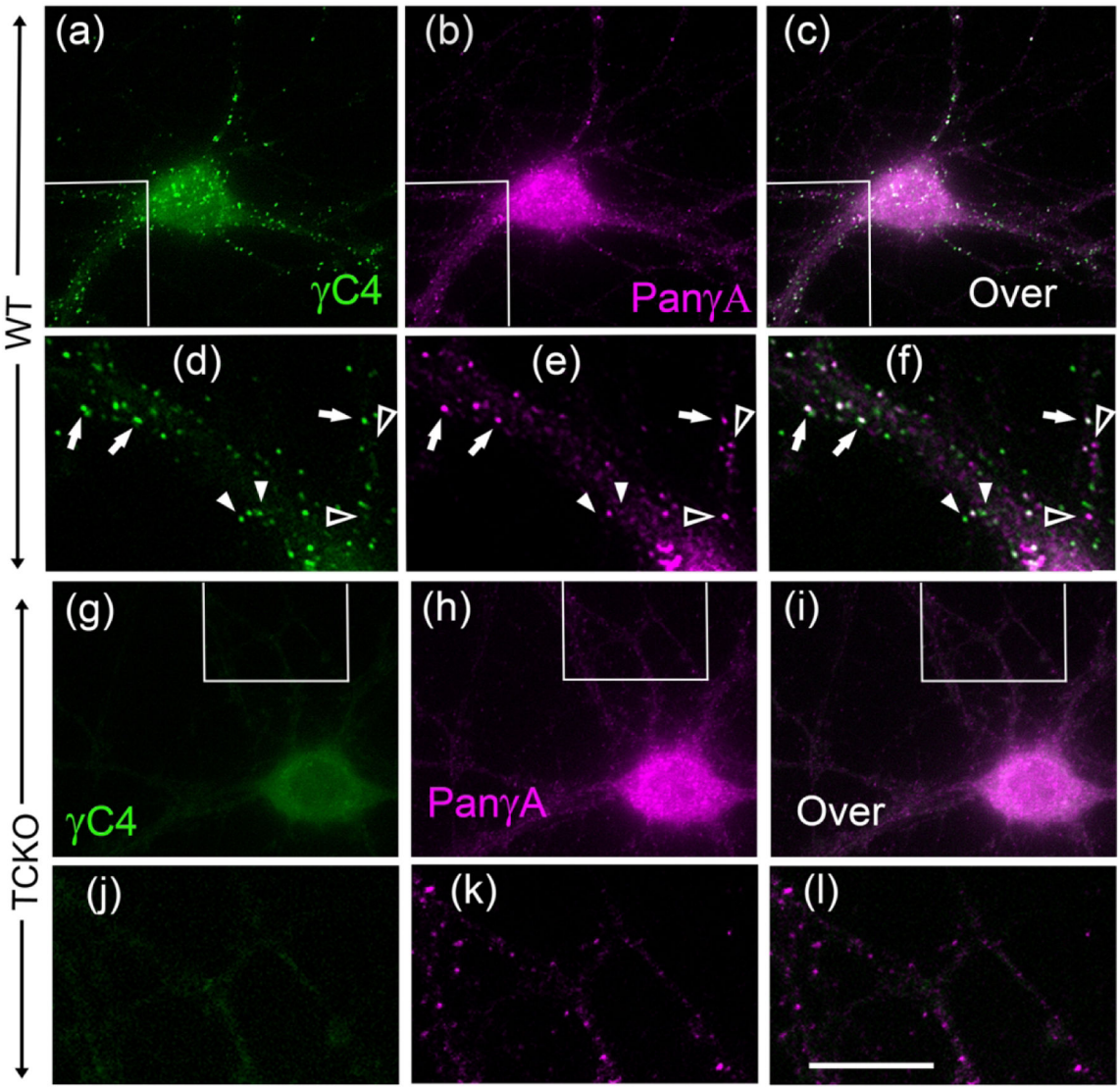

Fig. 6. Pcdh-γC4 expression in cultured HP neurons from WT and the TCKO mouse.

Double-label immunofluorescence. Boxed areas are shown at higher magnification underneath the corresponding panel. **(a-f)** double-label immunofluorescence of WT mouse neurons with the Rb anti-Pcdh-γC4 (green) and Ms pan-Pcdh-γA mAb (magenta). Panels c and f show the corresponding overlays (Over). Arrows show co-localization of Pcdh-γC4 and pan-Pcdh-γA puncta. Filled arrowheads point to Pcdh-γC4 puncta with no corresponding pan-Pcdh-γA puncta. Empty arrowheads show pan-Pcdh-γA puncta with no corresponding Pcdh-γC4 puncta. **(g-l)** TCKO mouse neurons do not have Pcdh-γC4 puncta (green) but have pan-Pcdh-γA puncta (magenta). Panels i and l show the corresponding overlays (Over). The scale bar represents 20 μm for a-c and g-i; and 8 μm for d-f and j-l.

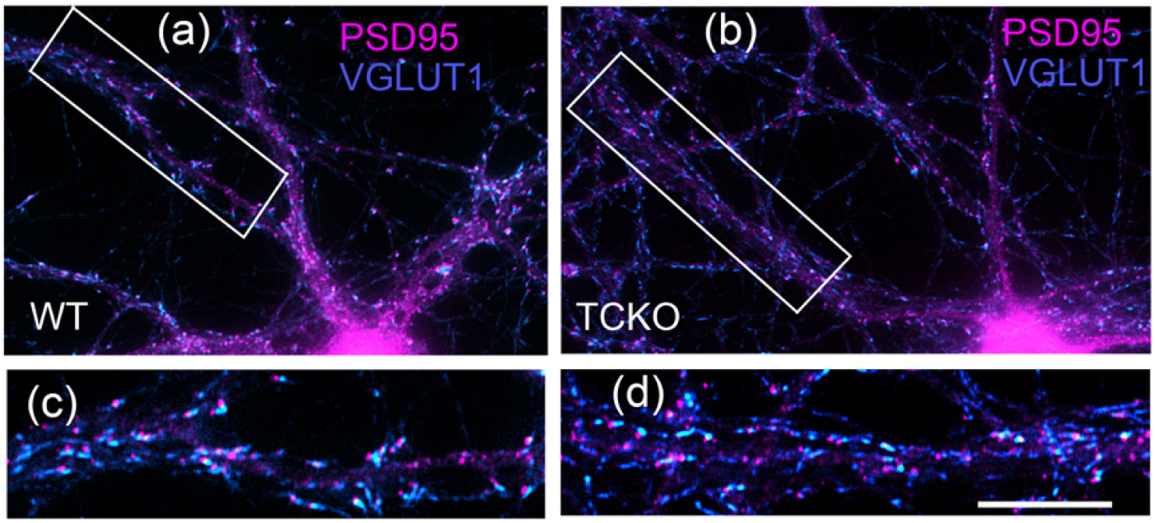

Fig. 7. The HP neurons of the TCKO mouse have many glutamatergic synaptic contacts comparable to the WT.

(a-d) Double-label immunofluorescence with Ms anti- PSD-95 (magenta) and GP anti-VGLUT1 (blue) in cultured hippocampal neurons from WT mouse (a and c) and TCKO mouse (b and d). Boxed areas in a and b are shown at higher magnification in c and d. Scale bar = 20 μm for a and b and 10 μm for c and d.

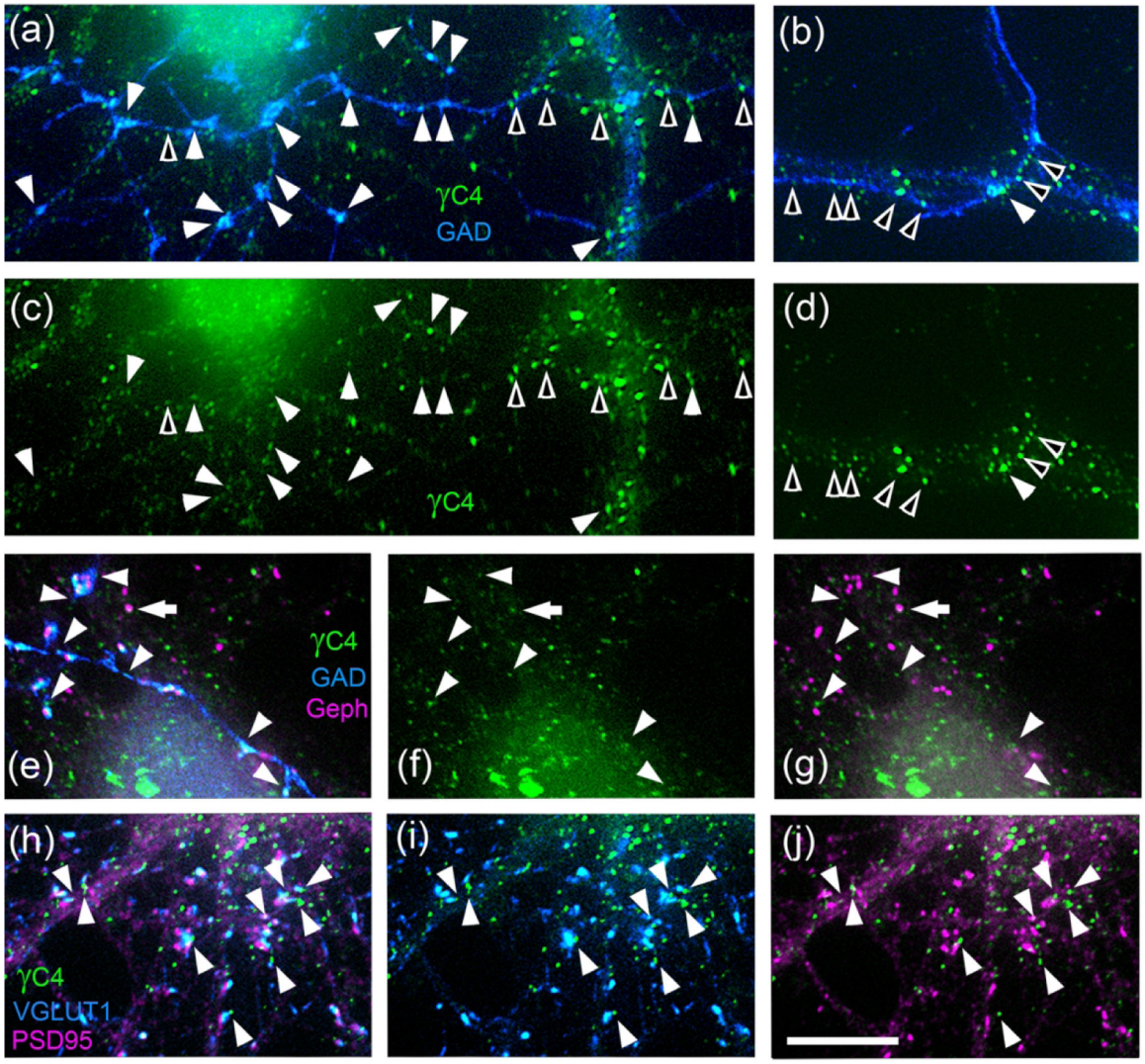

Fig. 8. Some Pcdh-γC4 puncta localize at contact points between axons and neurons, near synapses but not at synapses.

Rat hippocampal cultures. **(a-d)** Double-label immunofluorescence with Rb anti-Pcdh-γC4 (γC4, green) and sheep anti-GAD (blue). Arrowheads show Pcdh-γC4 puncta at contact points between an incoming axon and dendrites. Filled arrowheads show Pcdh-γC4 puncta associated with GAD+ boutons. Empty arrowheads show Pcdh-γC4 puncta associated with axon-neuron contacts but not boutons. Panels a and b show the overlays. Note than in a and c the GABAergic axon (blue) contacts a dendrite of a GABAergic interneuron (blue, right side of the panel) and a pyramidal neuron (left side of the panel). Panels b and d show an axon (blue) contacting a dendrite of a GABAergic interneuron (blue). Note that Pcdh-γC4 puncta associated or not associated with the axon are larger in the contacts with interneurons in a and b, than in the contacts with the pyramidal neuron in a. **(e-g)** Triple label immunofluorescence with Rb anti-Pcdh-γC4 (green), sheep anti-GAD (blue) and Ms anti-gephyrin (magenta). Some Pcdh-γC4 puncta are localized at contact points between the axon and neuron (arrowheads), however, the majority of these Pcdh-γC4 puncta are adjacent to, but seldom co-localize with (arrow), gephyrin clusters. **(h-j)** Triple label

immunofluorescence with Rb anti-Pcdh-γC4 (green), GP anti-VGLUT1 (blue) and Ms anti-PSD-95 mAb (magenta). Some Pcdh-γC4 puncta are associated with glutamatergic synapses (arrowheads) but the majority of Pcdh-γC4 puncta are adjacent to, but do not co-localize with VGLUT1 puncta or PSD-95 clusters. Scale bar = 10 μm.

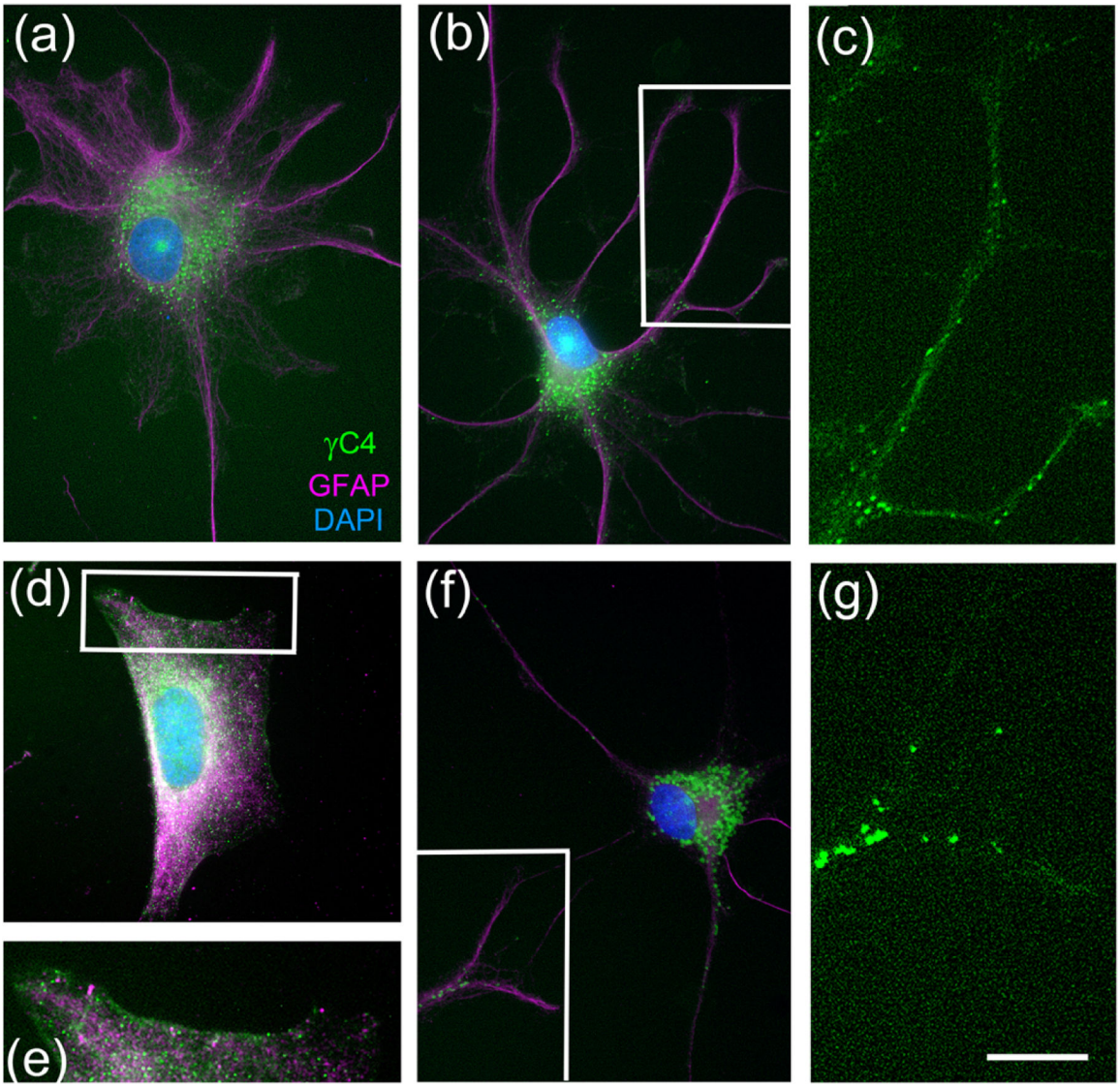

Fig. 9. Pcdh-γC4 is expressed by astrocytes forming puncta.

Triple-label immunofluorescence with Rb anti-Pcdh-γC4 (green), Ms anti-GFAP mAb (magenta) and DAPI (blue). Astrocytes with different morphologies are identified by anti-GFAP immunofluorescence. **(a-g)** Pcdh-γC4 puncta concentrate around the nucleus (a, b, d and f). Boxed areas in b, d and f are shown at higher magnification in c, e, and f respectively. Pcdh-γC4 immunofluorescence also associates with the plasma membrane (e) and with astrocyte processes (c and g). Scale bar represents 20 μm for a, b, d and f; and 10 μm for c, e and g.

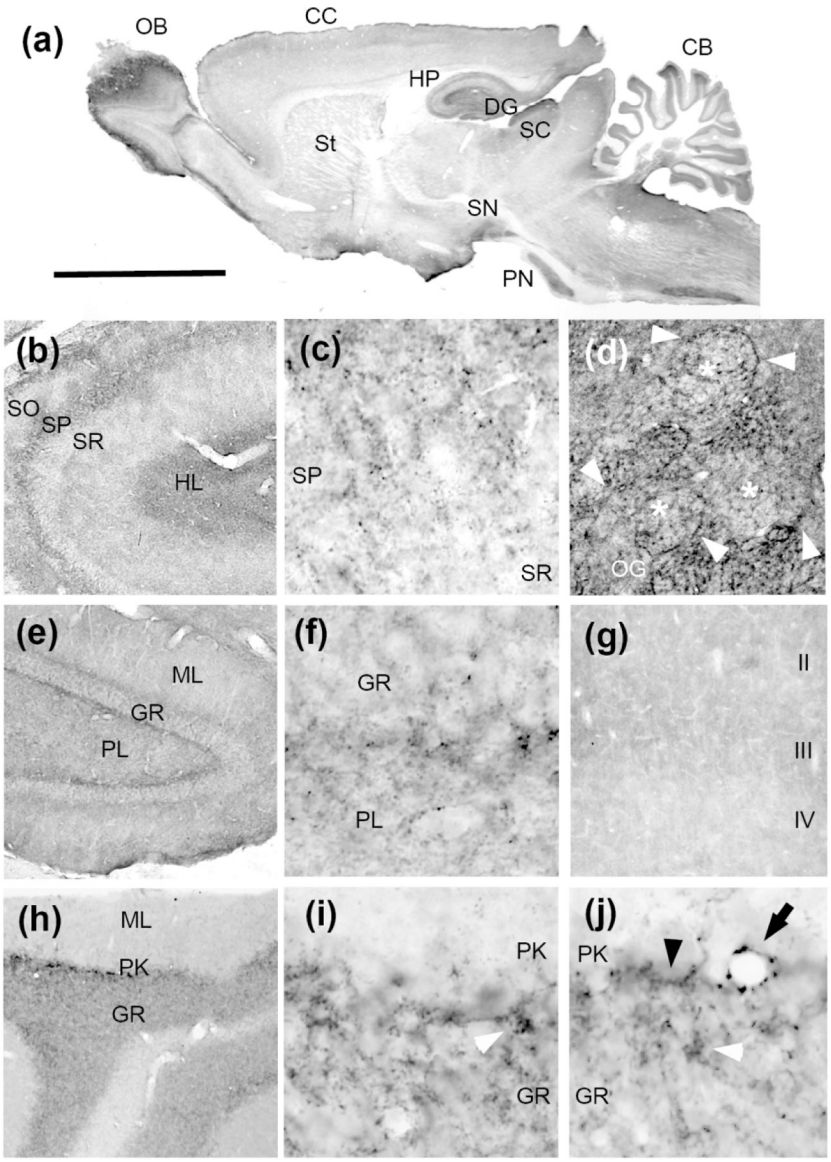

Fig. 10. Immunocytochemical localization of Pcdh-γC4 in the rat brain.

(a) Immunocytochemistry with anti-Pcdh-γC4 of a parasagittal section. **(b)** CA3 region of the HP. **(c)** Higher magnification of the boundary between the stratum pyramidale (SP) and stratum radiatum (SR) of the CA3 region of the HP. Note the granular aspect of the immunoreaction in the SP layer. **(d)** Olfactory glomeruli (OG) of the olfactory bulb. Asterisks indicate individual olfactory glomeruli. Arrowheads point to strong immunoreaction at the boundary surrounding the glomeruli **(e)** Dentate gyrus. **(f)** Higher magnification of the boundary between granule cell layer (GR) and the plexiform layer (PL) of the dentate gyrus. Note the granular aspect of the concentration of immunoreaction in the boundary. **(g)** Cerebral cortex, layers II-IV. **(h)** Cerebellum. **(I and j)** Higher magnification of the boundary between the Granule cell layer (GR) and Purkinje cell layer (PK). Granular accumulations of the immunoreaction occur in the GR layer (white arrowheads), in the boundary between Purkinje cells and the GR layer (black arrowheads) and surrounding

blood vessels (black arrow). Abbreviations: CB, cerebellum; CC, cerebral cortex; St, corpus striatum; DG, dentate gyrus; GR, granule cell layer; HL, hilus; HP, hippocampus; ML, molecular layer; OB, olfactory bulb; OG, olfactory glomerulus; Pn, pontine nuclei; PL, plexiform layer; PK, Purkinje cell layer; SO, stratum oriens; SP, stratum pyramidale; SR, stratum radiatum; SN, substantia nigra. Scale bar = 5 mm in a; 1 mm in b, e and h; 400 μm in g; 200 μm in d; and 100 μm in c, f, I and j.

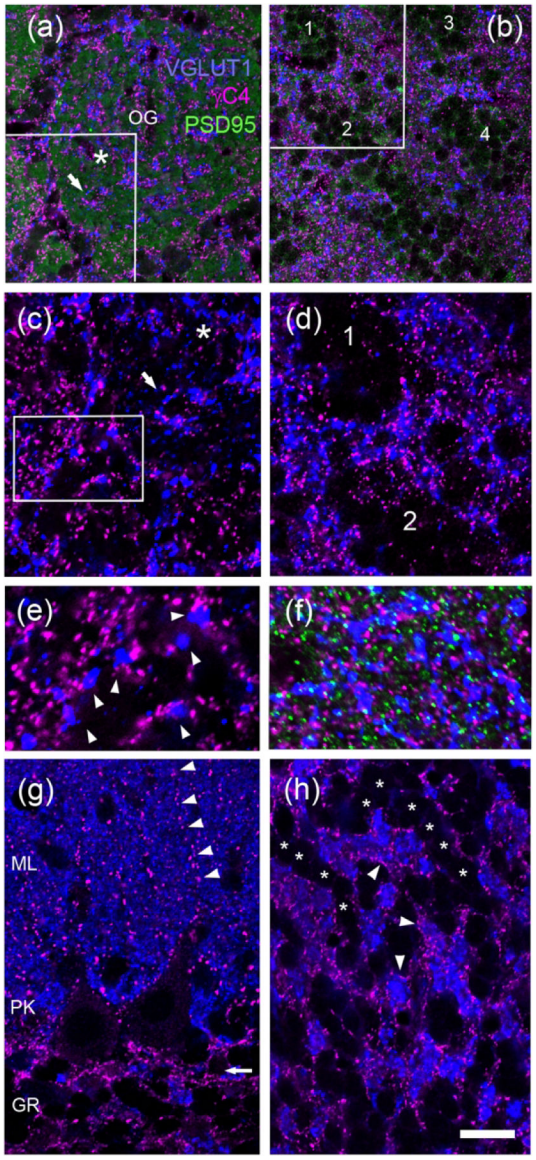

Fig. 11. In the rat olfactory bulb and cerebellum, Pcdh-γC4 forms puncta that are frequently localized adjacent to glutamatergic synapses.

(a, c and e) glomerular layer of olfactory bulb. **(b and d)** granule cell layer of olfactory bulb. **(f)** External plexiform layer of olfactory bulb. **(g and h)** cerebellum. All panels show immunofluorescence with Rb anti-Pcdh-γC4 (magenta) and GP anti-VGLUT1 (blue). Panels a, b and f also show Ms PSD-95 immunofluorescence (green). Boxed areas in a, b and c are shown at higher magnification in c, d and e respectively. Panel a is mostly occupied by an olfactory glomerulus labeled OG in the center. The asterisk in a and c are placed in the same position inside the OG to serve as a reference. The arrows in a and c point to the same VGLUT1 puncta inside the glomerulus, which are also associated with Pcdh-γC4 puncta. Arrowheads in e point to Pcdh-γC4 puncta associated with VGLUT1 terminals. Numbers in b and d indicate some granule cell aggregates in the olfactory granule layer. (g) In the cerebellum, the arrow indicates the region with the highest concentration of bright Pcdh-γC4 puncta, which is at the boundary between Purkinje cell layer (PK) and

granule cell layer (GR). Arrowheads point to a row of Pcdh-γC4 puncta in the molecular layer (ML). (h) Granule cell layer of the cerebellum. Asterisks indicate rows of granule cells. Note the absence of Pcdh-γC4 puncta in-between granule cells of the same row and the presence of Pcdh-γC4 puncta (arrowheads) separating VGLUT1 labeled synaptic glomeruli (blue) and granule cells. Scale bar represents 20 μm for a and b; 10 μm for c and d; 5 μm for e and f; and 12 μm for g and h.

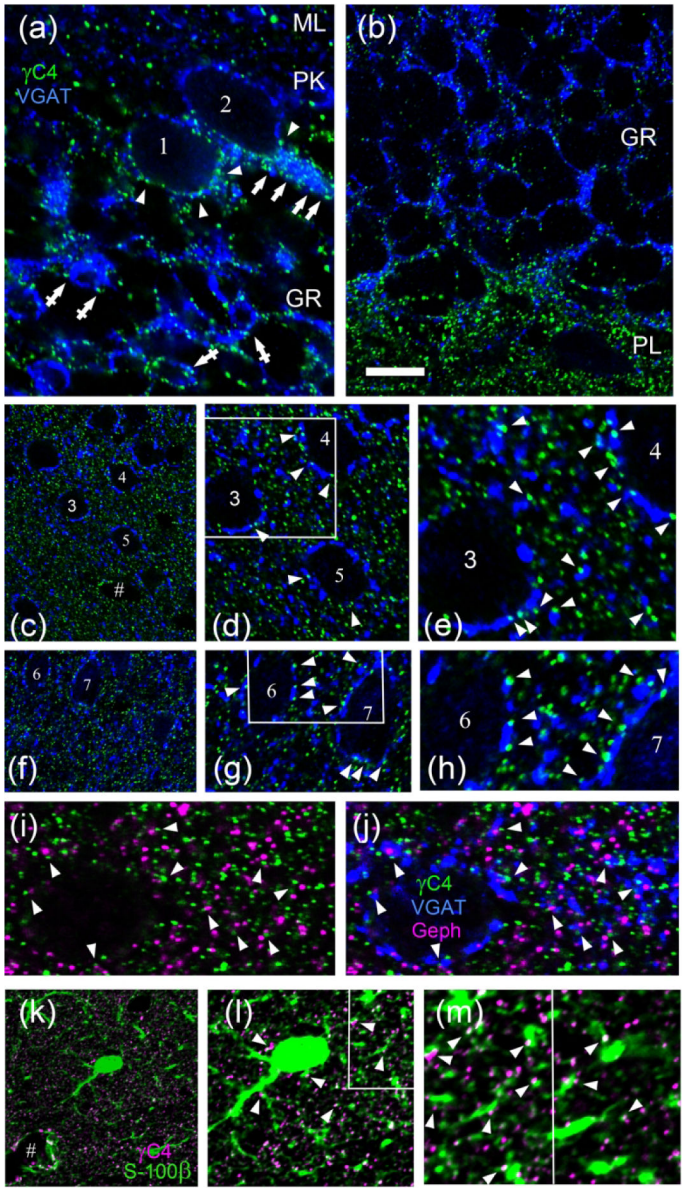

Fig. 12. Pcdh-γC4 puncta and are also frequently localized adjacent to GABAergic synapses.

(a-h) Double-label immunofluorescence with Rb anti-Pcdh-γC4 (green) and GP anti-VGAT (blue) in cerebellum (a), dentate gyrus (b) and layer III of cerebral cortex (c-h). Numbers indicate somas of some individual neurons. In a and b, the abbreviations for the layers are as defined in the legend to Fig 10. Arrowheads in a point to Pcdh-γC4 puncta associated with the soma of PK cells. Arrows in a point to Pcdh-γC4 puncta associated with the VGAT-containing pinceaux contacting the AIS of Purkinje cells. Crossed arrowheads in a point to Pcdh-γC4 puncta associated with VGAT-enriched synaptic glomeruli in the granule cell layer. Arrowheads in a, d, e, g and h point to Pcdh-γC4 puncta that are adjacent to VGAT terminals. **(i and j)** Triple-label immunofluorescence with Rb anti-Pcdh-γC4 (green) and GP anti-VGAT (blue) and Ms Geph (magenta) in layer III of the rat cerebral cortex. Arrowheads in i and j point to Pcdh-γC4 puncta that are adjacent to GABAergic synapses.

(k-m) Double-label immunofluorescence with Rb anti-Pcdh-γC4 (magenta) and Ms anti-S100β (green). Arrowheads in l and m point to Pcdh-γC4 puncta associated with S-100β-labeled astrocyte processes. The symbol # indicates blood vessels in c and k. Boxed areas in d, g and l are shown at higher magnification in e, h and the left side of m respectively. Scale bar represents 10 μm for a, b, d, g and l; 20 μm for c, f and k; 5 μm for e, h and m; and 4.4 μm for i and j.

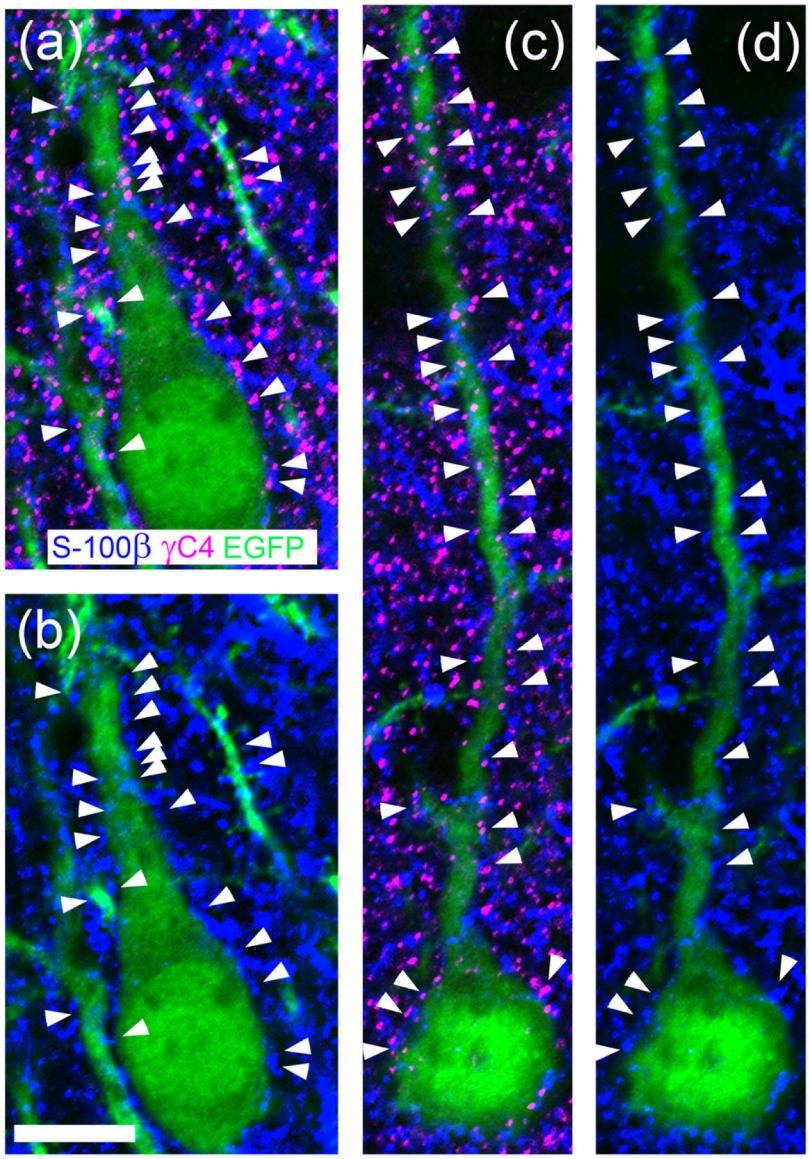

Fig. 13. Pcdh-γC4 puncta frequently are associated with contacts between neurons and astrocyte processes in the cerebral cortex.

(a and c) triple-label immunofluorescence with Rb anti-Pcdh-γC4 (magenta), Ms anti-S100β (blue) and Chicken anti-GFP (green) of the cerebral cortex of a P35 rat that had been *in utero* electroporated with EGFP. The EGFP immunofluorescence (green) reveals two transfected pyramidal neurons of layer III expressing EGFP. Astrocyte processes are identified by S100β immunofluorescence (blue). **(b and d)** correspond to a and c respectively, in which the magenta channel has been eliminated to better appreciate the localization of the Pcdh-γC4 puncta (arrowheads) at contacts between astrocyte processes (blue) and pyramidal neurons (green). Scale bar = 10 μm.

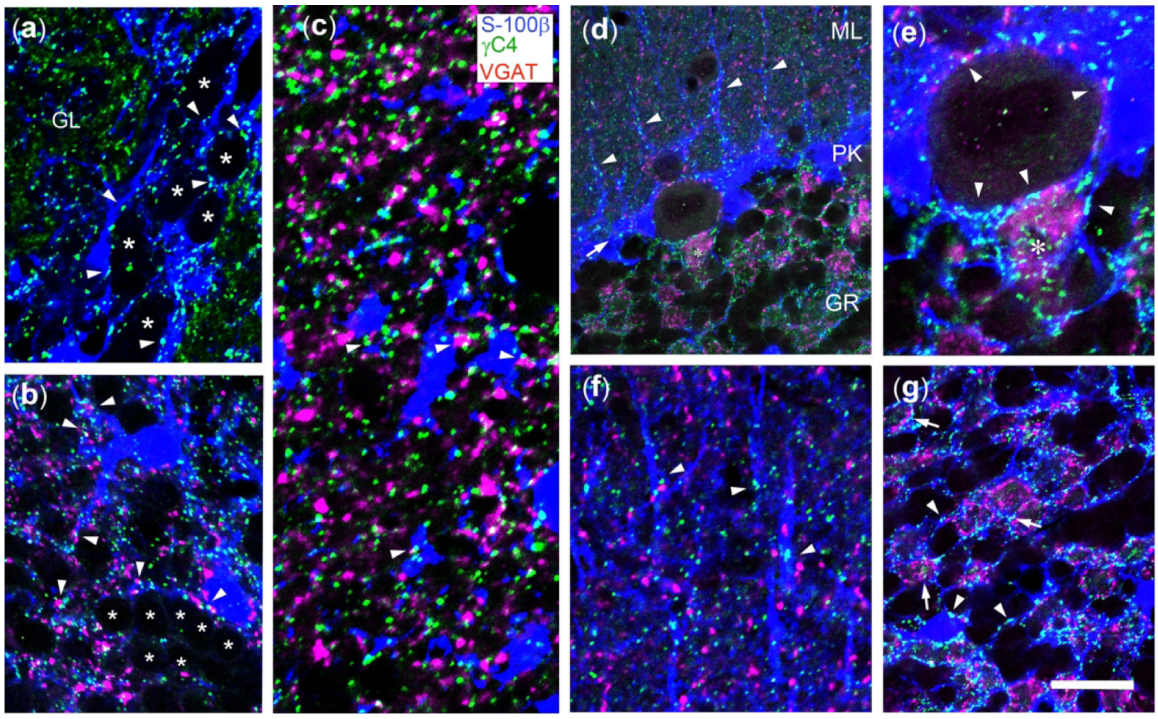

Fig. 14. Pcdh-γC4 puncta frequently are associated with contacts between astrocytes (or Bergmann glia) and neurons in the olfactory bulb and cerebellum, frequently apposed to synapses.

Triple-label immunofluorescence with Rb anti-Pcdh-γC4 (green), GP anti-VGAT (magenta) and Ms anti-S100β (blue). **(a)** Glomerular layer of the olfactory bulb. Pcdh-γC4 puncta are present at the contacts (arrowheads) between periglomerular astrocytes (blue) and periglomerular neurons (asterisks). Pcdh-γC4 puncta are also present inside the glomerulus. **(b)** Granule cell layer of the olfactory bulb. Pcdh-γC4 puncta concentrate on contacts (arrowheads) between astrocytes (soma and processes) and neurons, frequently apposed to VGAT-containing terminals. Note the row of granule neurons (asterisks). Pcdh-γC4 puncta are largely absent from the contacts granule cell to granule cell. **(c)** External plexiform layer of the olfactory bulb. Pcdh-γC4 puncta are frequently associated with astrocyte processes and VGAT puncta (arrowheads). **(d)** Cerebellum. The abbreviations for the layers are as defined in the legend to Fig 10. Note the presence of Bergmann glia cell bodies on the PK layer (arrow), their radial fibers in the ML and the associated Pcdh-γC4 puncta (arrowheads). **(e)** Purkinje cells, also shown in d, are extensively surrounded by Bergmann glia (blue). There are Pcdh-γC4 puncta in the contacts between these Purkinje cells and Bergmann glia (arrowheads). Pcdh-γC4 puncta also associate with the VGAT-containing pinceaux (magenta, asterisk) and astrocyte processes in the AIS of the Purkinje cell. **(f)** Radial Bergmann glia fibers in the ML of the cerebellum have associated Pcdh-γC4 puncta, often associated with VGAT terminals. **(g)** Granule cell layer of the cerebellum. Note the astrocytic processes (blue) surrounding the VGAT-containing synaptic glomeruli (magenta) and the Pcdh-γC4 puncta (green) associated with the synaptic glomeruli (arrows). Pcdh-γC4 puncta are also present in the contacts between astrocyte processes and granule cells

(arrowheads). Scale bar = 10 μm in a; 11.5 μm in b; 5.5 μm in c; 20 μm in d; 13 μm in e and f; and 17 μm in g.

Table I.

Primary Antibodies

Antigen	Immunogen	Manufacturer	Dilution
Pcdh-γC4	Synthetic peptide (DHAPRFPRQQLDLE) AA 128–141 of rat Pcdh-γC4	Made in our laboratory, Rabbit polyclonal	1:150[1] 1:30 to 1:50[2] 1:600[3] 1:100[4] 1:25[5]
Pan-Pcdh-γ	AA 808–931 (C-terminal constant domain) of mouse Pcdh-γA1	NeuroMab, Cat# 73–185, Lot# 437–3VA-24, RRID:AB_10676098; mouse monoclonal, clone N159/5.	1:15[2,3]
Pan-Pcdh-γA	AA 720–804 (variable cytoplasmic domain) of mouse Pcdh-γA3	NeuroMab, Cat#73–178, Lot# 437–3VA-12, RRID:AB_10672982; mouse monoclonal, clone N144/32.	1:15[2]
Pcdh8	AA 1–149 of human Pcdh8	Santa Cruz, Cat# SC-377348, Lot# 3E1817; RRID:AB_2259153; mouse monoclonal, clone D7.	1:50[1] 1:100[3]
gephyrin	Affinity-purified rat glycine receptor protein complex. N-terminus surrounding phospho-serines 268 and 270	Synaptic Systems; Cat # 147021; Lot# 147021/9; RRID:AB_1279448; Mouse; Monoclonal clone mAb7a.	1:200[1,2]
GAD65	purified rat GAD	Dr. Irwin J. Kopin; lot#1440–4; RRID:AB_2314493; Sheep; Polyclonal.	1:600[2]
GFAP	Bovine spinal cord homogenate	PharMingen, Cat# 60311D, Lot# MO50728; RRID:AB_2313650; mouse monoclonal, clone 4A11.	1:600[2]
PSD-95	GST fusion protein encoding the full-length rat PSD-95	Chicken polyclonal antiserum UCT-C1, gift from Dr. Randall S. Walikonis.	1:1,000[1]
PSD-95	Recombinant rat PSD-95	Millipore, Cat# MAB 1596, Lot# LV1453199, RRID:AB_2092365; mouse monoclonal, clone 6G6–1C9.	1:100[1,2]
vGAT	Synthetic peptide SLEGLIEAYRTNAED of rat VGAT	Synaptic Systems, Cat# 131004; lot # 131004/13, RRID:AB_887873; Guinea pig polyclonal.	1:1,000 to 1:2,000[1]
vGlut1	Synthetic peptide GATHSTVQPPRPPPPVRDY of rat vGLUT1	Chemicon, Cat# AB5905; Lot# 24080852, RRID:AB_2301751; Guinea pig polyclonal.	1:10,000[1,2]
S-100β	Purified bovine brain S-100β preparation	Sigma, Cat# S2532; Lot# 085K4880 and AB4200671, RRID:AB_477499; clone SH-B1, mouse monoclonal.	1:500–1:2,000[1]
Actin	Purified chicken gizzard actin	Millipore, Cat# MAB1501; Lot # LV1547855; RRID:AB_2223041; clone C4, mouse monoclonal.	1:1,000[5]

[1] IF with brain slices

[2] IF with neuronal or glial cultures

[3] IF with HEK293 cells

J Comp Neurol. Author manuscript; available in PMC 2021 April 01.

4 ICC with brain slices

5 Immunoblot